Article:
Reyhani Haghighi, S., Cazzonelli, C.I., Hartley, S.E. et al. (2026) Elevated UV-B alters anti-herbivore plant defence allocation, while silicon supplementation maintains resistance. Functional Ecology. ISSN: 0269-8463

https://doi.org/10.1111/1365-2435.70398

Received: 3 March 2026 | Accepted: 3 June 2026

DOI: 10.1111/1365-2435.70398

Functional Ecology

RESEARCH ARTICLE

Elevated UV-B alters anti-herbivore plant defence allocation, while silicon supplementation maintains resistance

Sajjad Reyhani Haghighi[1] | Christopher I. Cazzonelli[1] | Sue E. Hartley[2] | Scott N. Johnson[1]

[1]Hawkesbury Institute for the Environment, Western Sydney University, Penrith, New South Wales, Australia

[2]School of Biosciences, University of Sheffield, Sheffield, UK

Correspondence
Sajjad Reyhani Haghighi
Email: s.reyhanihaghighi@westernsydney.edu.au; sajjad.reyhani1408@gmail.com

Handling Editor: James Michael William Ryalls

Abstract

1. The impacts of elevated surface ultraviolet-B (UV-B) on ecological processes, such as anti-herbivore defence in plants, remain poorly understood. Many cereal crops depend on accumulating silicon (Si) in their tissues to resist insect herbivory. UV-B is known to affect oxidative signalling, which is an early signal triggered by herbivore attack and hence could potentially impact upon subsequent defence allocation.
2. We tested how UV-B light, Si supplementation and herbivory interact to impact plant defence and insect performance. We conducted a fully factorial glasshouse experiment using hydroponically grown wheat (*Triticum aestivum*), manipulating three UV-B levels (low, moderate and high) and Si supply, before subjecting plants to herbivory by *Helicoverpa armigera*.
3. Elevated UV-B increased oxidative signalling (+52%) and antioxidant capacity but slightly reduced foliar Si accumulation (−8.6%). Silicon supplementation reduced lipid peroxidation and altered defence allocation, lowering UV-B- and herbivory-induced phenolic production while increasing polyphenol oxidase activity and Si concentration. Phenolics increased under elevated UV-B (up to +13%), and herbivory increased phenolics only in plants without Si supplementation (up to +30%). Under herbivory, Si reduced phenolic levels (17% lower than −Si plants) and suppressed phenolic induction by 25%.
4. Larvae feeding on Si-supplemented plants showed a 35% reduction in growth rate, which persisted despite UV-B-driven reductions in foliar Si. High UV-B depleted larval energy reserves, with carbohydrate levels declining by 52%, alongside reduced lipid and triglyceride stores and a 40% increase in protein. Silicon altered larval energy allocation, increasing carbohydrate reserves (2.5-fold) and glycogen (up to 2.9-fold), while larvae feeding on −Si plants retained higher lipid and triglyceride stores.
5. Collectively, these results demonstrate that Si helps maintain plant resistance under simultaneous UV-B exposure and herbivory by altering defence investment and increasing metabolic costs to herbivores. These findings provide broader implications

for understanding how crops maintain resistance under future changes in UV-B light conditions.

KEYWORDS
herbivory, induced resistance, multitrophic interactions, oxidative stress, plant defence, silicon supplementation, *Triticum aestivum*, ultraviolet-B

1 | INTRODUCTION

Global change is altering the abiotic and biotic conditions under which staple crops grow, with consequences for agricultural productivity and food security. Surface ultraviolet-B (UV-B) exposure remains ecologically relevant because it is influenced by stratospheric ozone and atmospheric conditions, and can reduce growth, yield and stress tolerance in cereals, such as wheat, rice and maize (Correia et al., 2000; Liaqat et al., 2023; Teramura & Sullivan, 1994). Although stratospheric ozone is recovering under the Montreal Protocol, total column ozone remains ~2–5% below 1964–1980 levels, with return to 1980 baselines projected around the 2040s globally and later at some mid-latitudes (World Meteorological Organization, 2022). Concurrently, herbivory pressure is expected to intensify under climate change, with meta-analyses reporting increased consumption rates, particularly in grass- and cereal-dominated systems (Hamann et al., 2021; Liu et al., 2024; Zvereva & Kozlov, 2006).

UV-B acts as both a stressor and a regulatory signal. At ecologically relevant intensities, UV-B is perceived via the UVR8 photoreceptor and triggers redox-based signalling that elevates antioxidant capacity and induces phenylpropanoid-associated defences, including the accumulation of phenolics that function as UV screens and ROS scavengers, and activation of defence enzymes, such as phenylalanine ammonia-lyase (PAL) and polyphenol oxidase (PPO) (Chen et al., 2022; Hideg et al., 2013; Shi & Liu, 2021). The intensity of UV-B exposure influences the magnitude of these responses, with implications for how plants balance defence investment against growth (Chen et al., 2022; Escobar-Bravo et al., 2021). These responses are closely linked to changes in oxidative status, including variation in reactive oxygen species (ROS), such as hydrogen peroxide (H_2O_2) and downstream lipid peroxidation (Chen et al., 2022; Hideg et al., 2013; Shi & Liu, 2021). UV-B-induced responses overlap with herbivory-associated signalling, and jasmonic acid (JA)-mediated pathways can amplify defence induction under combined stress (Demkura et al., 2010; Izaguirre et al., 2007; Qi et al., 2018). How cereals allocate resources between competing defence strategies under co-occurring UV-B exposure and herbivory remains poorly resolved.

Grasses also rely heavily on Si-based defences against herbivores. Si is taken up from the soil solution and deposited in epidermal tissues, where it strengthens cell walls and deters herbivores through both physical and chemical mechanisms, reducing digestibility through abrasion, accelerated mandible wear and silicification-mediated impedance of digestive enzyme access to cell contents (Hartley & DeGabriel, 2016; Massey & Hartley, 2009; Van Soest & Jones, 1968). In addition to this, Si can alleviate UV-B stress by enhancing antioxidant capacity and limiting oxidative damage, including reductions in ROS accumulation and lipid peroxidation (Goto et al., 2003; Malčovská et al., 2014; Shen, Li, et al., 2010; Tripathi et al., 2017). Si accumulation may also provide a metabolically cheaper alternative to carbon-based constituents, including phenolic defences (Cooke & Leishman, 2012; Frew et al., 2016). Trade-offs between Si and phenolic defences are well documented under herbivory and elevated CO_2, where increased carbon availability enhances phenolic investment, but Si supplementation suppresses it (Biru et al., 2021; Cooke & Leishman, 2012; Johnson & Hartley, 2018; Schaller et al., 2012). However, Si can also enhance phenolic metabolism in other stress contexts, including pathogen or fungal attack (Fauteux et al., 2006), indicating that Si does not uniformly suppress phenolics. Under UV-B stress, the direction of Si–phenolic interactions is less certain, as existing studies report contrasting outcomes (Goto et al., 2003; Malčovská et al., 2014). Such shifts in defence allocation can also modify foliar nutritional quality, including concentrations of carbohydrates, free amino acids (FAAs) and protein, with downstream consequences for herbivore nutrition and performance (Frew et al., 2016; Robinson et al., 2012; Zvereva & Kozlov, 2006). Whether Si similarly reconfigures defence allocations under UV-B exposure—particularly in the presence of herbivory—remains unclear.

Changes in plant defence chemistry and nutritional quality can propagate to herbivores, altering performance and energy allocation (Robinson et al., 2012; Zvereva & Kozlov, 2006). Phenolic-rich diets can impose oxidative challenges on herbivores through pro-oxidant activity and increased detoxification demands, elevating ROS and lipid peroxidation and requiring compensatory antioxidant investment (R. V. Barbehenn et al., 2008; Lalouette et al., 2011; War et al., 2012). At the same time, shifts in key nutritional pools—particularly soluble carbohydrates, FAAs and protein—can modify nutrient assimilation and drive trade-offs in allocation among short-term reserves (carbohydrates and glycogen) and longer-term storage (lipids and triglycerides), with consequences for growth and survival (Lee et al., 2008; Raubenheimer et al., 2009; Simpson et al., 2015). Despite evidence for independent effects of UV-B and Si on plant traits, their combined influence on defence allocation and herbivore oxidative and metabolic physiology remains poorly characterised.

Global agriculture currently faces spatially variable and episodically elevated UV-B exposure combined with likely increases in herbivore pressure under a warming climate, yet how staple crops, such as wheat allocate resources between

competing defence strategies under these conditions, remains poorly resolved. To address this, we implemented a fully factorial experiment crossing Si supplementation (±Si), UV-B intensity (low, moderate and high) and herbivory (±*Helicoverpa armigera*) to quantify foliar Si accumulation, oxidative and antioxidant status, phenylpropanoid-associated defences and downstream herbivore growth, redox physiology and energy allocation (Figure 1). We used *Helicoverpa armigera*, a globally important polyphagous crop pest (Kriticos et al., 2015), to assess plant-mediated effects on herbivores at the next trophic level. We hypothesised that: (H_1) increasing UV-B elevates oxidative signalling in wheat, inducing antioxidant and phenylpropanoid-associated defence pathways; (H_2) Si supplementation buffers UV-B-associated oxidative damage, increases foliar Si and shifts defence investment away from phenolic accumulation towards Si-based resistance; (H_3) UV-B and herbivory generate additive or non-additive effects on oxidative and defence traits that depend on Si supply; and (H_4) these plant responses cascade to herbivores, suppressing growth and altering redox physiology and energy allocation (Figure 1).

2 | MATERIALS AND METHODS

2.1 | Experimental design

We conducted a fully factorial glasshouse experiment to test how UV-B radiation, Si supplementation, herbivory and their interactions affect wheat physiology and herbivore performance. Wheat (*Triticum aestivum* L., cv. 'Catapult') plants were assigned to 12 treatment combinations (3 UV-B levels × 2 Si levels × 2 herbivory levels) with 15 biological replicates each ($n = 180$ hydroponic units).

2.2 | Plant material and seed preparation

Seeds were surface-sterilised in 0.9% (v/v) sodium hypochlorite with 0.1% (v/v) Triton X-100 for 30 min, rinsed five times with Milli-Q water and placed on perlite moistened with Milli-Q water. Seeds were germinated in the glasshouse for 2 weeks and then

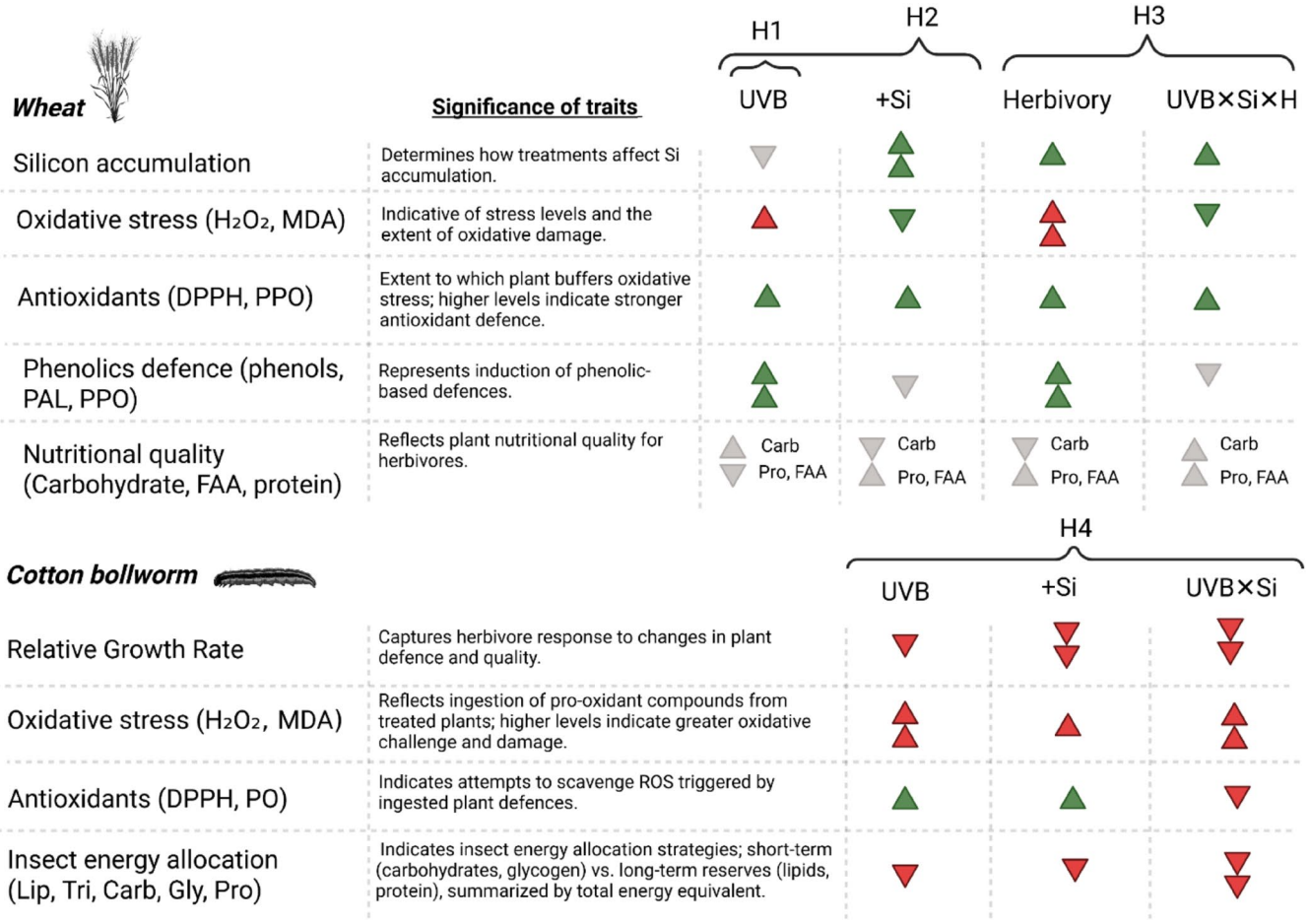

FIGURE 1 Summary of predicted responses of wheat plants and *Helicoverpa armigera* larvae to increasing ultraviolet-B (UV-B) exposure, silicon supplementation, herbivory and their interactions. Arrows indicate expected changes in traits under hypotheses (H_1–H_4). Single triangles show moderate effects, double triangles indicate stronger effects, and grey triangles suggest trade-offs or context-dependent responses. Green triangles denote beneficial outcomes, while red triangles indicate negative ones. The middle column highlights the functional significance of each trait.

transplanted into individual hydroponic units (Islam et al., 2023). The glasshouse was maintained at 24/18°C (day/night) under a 16 L:8D photoperiod cycle and 60 ± 5% relative humidity. Each hydroponic unit comprised two nested plastic cups containing 450 mL of a modified full-strength nutrient solution, following Hall et al. (2020). Nutrient solutions were replaced weekly for the first 2 weeks and biweekly thereafter. Plants were grown hydroponically for a further 6 weeks before herbivory assays (Hall et al., 2020). For the plant's biochemical traits, we analysed a random subsample of six plants per treatment combination. Si concentrations were quantified on all available replicates.

2.3 | Silicon supplementation

Si was supplied in the +Si treatments as 2 mM potassium silicate (K_2SiO_3; Agsil32®, PQ Australia), adjusted to pH 5.5 with HCl to minimise silicate polymerisation (Ma & Yamaji, 2006). Control plants (-Si) received KCl (Sigma-Aldrich, MO, USA) to match the added K^+ from K_2SiO_3 (Hall et al., 2020).

2.4 | UV-B treatments

To simulate biologically relevant exposure, we applied a three-level UV-B gradient informed by regional solar irradiance using the Australian Bureau of Meteorology UV Index (see Supplementary Material) and verified by direct spectroradiometric measurement. Unweighted irradiance ($W\,m^{-2}$) and daily dose ($kJ\,m^{-2}\,d^{-1}$) at canopy height were: low $0.1\,W\,m^{-2}$ ($1.8\,kJ\,m^{-2}\,d^{-1}$), moderate $0.26\,W\,m^{-2}$ ($4.62\,kJ\,m^{-2}\,d^{-1}$) and high $1.15\,W\,m^{-2}$ ($20.7\,kJ\,m^{-2}\,d^{-1}$). Biologically effective doses, calculated by weighting measured spectra against the generalised plant action spectrum (Flint & Caldwell, 2003), scaled proportionally with unweighted irradiance across treatments (Figure S3). UV-B was delivered via MIGRO UV-B 310 lamps (MIGRO, Dublin, Ireland; peak 310 nm), with exposure running from 10:00 to 15:00 daily ($5\,h\,d^{-1}$). Supplemental PAR was provided by TSL2000 LED fixtures (Mars Hydro, Shenzhen, China), delivering no detectable UV-B and a consistent PPFD of $550\,\mu mol\,m^{-2}\,s^{-1}$ at canopy height across all UV-B treatments. UV-B irradiance (280–315 nm) was measured using an LS125 meter with a UVB-X0 probe (Linshang Technology, Shenzhen, China) and verified by high-resolution scans using a PS-300 spectroradiometer (Apogee Instruments, Logan, UT, USA; spectral profiles and stability checks are shown in Figures S1 and S2). To eliminate background UV interference, the glasshouse was lined with UV-opaque polymer curtains; spot measurements confirmed >90% attenuation of ambient UV-B and daytime background $<0.003\,W\,m^{-2}$. UV-B spatial variability within each treatment was <12% CV at canopy height. Plants were rotated twice weekly within UV-B treatments. UV-B treatments were reassigned among benches weekly, with irradiance adjusted to maintain the target dose (verified using an LS125 UVB-X0). This design minimised bench effects while ensuring each plant received only its assigned UV-B level.

2.5 | Herbivory treatment

Wheat plants were inoculated with a single third-instar *Helicoverpa armigera* larva, which was starved for 24 h prior to application. The larvae were sourced from egg discs provided by CSIRO Agriculture & Food (Narrabri, Australia) and reared on an artificial diet until reaching the third instar. Following inoculation, the larvae were confined to the wheat shoots with transparent Perspex sheaths, allowing herbivores to feed on the shoot parts of the plants for a week. Subsequently, the larvae were collected for further relative growth rate calculation and biochemical analysis. To isolate plant-mediated effects of UV-B, all *H. armigera* bioassays were conducted after UV exposure had ended. This approach avoids direct UV-B impacts on insects, ensuring that observed responses reflect UV-B- and Si-induced changes in host plant traits. Under ecologically realistic conditions, many herbivores can actively avoid harmful UV-B by retreating to the lower leaf surface (Ohtsuka & Osakabe, 2009). Accordingly, post-exposure designs have been widely adopted to disentangle direct and indirect effects of UV-B (Demkura et al., 2010; Escobar-Bravo et al., 2021; Nocchi et al., 2020; Prieto-Ruiz et al., 2019; Qi et al., 2018).

2.6 | Plant biochemical analyses

2.6.1 | Foliar silicon

All leaves per plant were harvested and oven-dried (60°C, 3 days) and pooled during ball-milling; 80 mg of the resulting powder was analysed for Si concentration by X-ray fluorescence (Epsilon 3X, PANalytical) following Reidinger et al. (2012). Calibration used certified reference material NCS ZC73018 (Citrus leaves). Results are expressed as % Si (DW).

2.6.2 | Oxidative stress and antioxidant capacity

H_2O_2 content was quantified from 0.10 g of fresh tissue (Velikova et al., 2000). Tissue was homogenised in 0.1% (w/v) trichloroacetic acid (TCA), centrifuged (12,000 × g, 15 min, 4°C) and the supernatant was mixed with 10 mM potassium phosphate buffer (pH 7.0) and 1 M KI. Absorbance at 390 nm was read against reagent blanks, converted from a standard curve and expressed as $\mu mol\,g^{-1}$ fresh weight (FW).

MDA was determined by thiobarbituric-acid reactivity (Sunkar et al., 2006). Leaf tissue (0.1 g) was homogenised in 0.1% TCA and reacted with 0.5% TBA in 20% TCA, heated (95°C, 30 min), cooled on ice and centrifuged (10,000 × g, 10 min). Absorbance was measured

at 532 and 600 nm. Malondialdehyde (MDA) concentration was calculated using $\varepsilon = 155\,mM^{-1}\,cm^{-1}$ and expressed as μmol g^{-1} FW.

Antioxidant capacity was assessed by DPPH radical scavenging (Molyneux, 2004). Fresh tissue (0.1 g) was homogenised in 1.0 mL 80% (v/v) methanol and centrifuged (12,000 × g, 10 min). An aliquot (100 μL) was mixed with 900 μL 0.1 mM DPPH (methanol) and incubated 30 min in the dark at room temperature, and A_{517} was recorded against methanol/DPPH blanks (Brand-Williams et al., 1995; Molyneux, 2004). Percent inhibition was calculated as follows:

$$\%\,\text{Inhibition} = \left(\frac{A_{\text{control}} - A_{\text{sample}}}{A_{\text{control}}}\right) \times 100$$

where $A_{control}$ is the absorbance of the DPPH solution without extract, and A_{sample} is the absorbance with the extract.

2.6.3 | Phenolic defence pathways (total phenolics, PAL, PPO)

PPO activity (EC 1.10.3.1) was assayed with L-DOPA in 160 mM phosphate buffer (pH 6.8); dopachrome formation was read at 475 nm ($\varepsilon = 3600\,M^{-1}\,cm^{-1}$; Duckworth & Coleman, 1970; Yoruk & Marshall, 2003) and expressed as μmol $min^{-1}\,g^{-1}$ FW. Total phenolics followed Ainsworth and Gillespie (2007): 0.10 g tissue was extracted in 95% methanol (48 h, dark), centrifuged (13,000 × g, 5 min) and reacted with 10% (v/v) Folin–Ciocalteu and 700 mM Na_2CO_3 (2 h), and A_{765} was compared with gallic-acid standards; values are reported as mg gallic acid g^{-1} FW. PAL activity (EC 4.3.1.24) was quantified from (E)-cinnamic acid formation using 50 μL enzyme extract and 0.5 mL 30 mM L-phenylalanine in 50 mM Tris–HCl (pH 8.8), incubated at 37°C for 1 h and read at 290 nm ($\varepsilon = 9.5\,mM^{-1}\,cm^{-1}$), expressed as μmol $min^{-1}\,g^{-1}$ FW (Wang et al., 2006).

2.6.4 | Nutritional quality (protein, free amino acids, total soluble carbohydrates)

Protein was quantified by the Bradford (1976) assay (A_{595}) using a BSA standard curve. Fresh leaf (0.10 g) was homogenised in 50 mM potassium phosphate (pH 7.0) with 1% (w/v) PVP and 0.1 mM EDTA, and centrifuged (10,000 × g, 15 min, 4°C), and the supernatant (50 μL) was mixed with 1.5 mL Bradford reagent, incubated 20 min at room temperature and read against reagent blanks; results are expressed as mg g^{-1} FW.

Free amino acids were measured by the ninhydrin assay (Yemm et al., 1955). Leaves (0.10 g) were extracted in 600 μL 80% ethanol and centrifuged (16,000 × g, 20 min, 4°C); 200 μL extract was combined with 7.6 mL reagent (1% ninhydrin, 0.5 M citrate buffer pH 5.5, 87% glycerol; 5:2:12) and heated at 95°C for 30 min, and A_{570} compared with glycine standards; values are reported as mg g^{-1} FW.

Total soluble carbohydrates (TSC) were determined by the anthrone method (Yemm & Willis, 1954). The supernatant was mixed with anthrone (2 g L^{-1} in 96% H_2SO_4), chilled on ice for 10 min, heated at 100°C for 20 min and cooled to room temperature, and A_{625} compared with D-glucose standards; TSC is expressed as mg g^{-1} FW.

2.7 | Insect analyses

2.7.1 | Insect performance

For herbivory-treated plants ($n = 90$; 3 UV-B × 2 Si × 15 replicates), third-instar *H. armigera* were starved for 24 h to clear frass, weighed, allowed to feed in situ for 7 d and re-weighed. Individuals that died or were lost before final weighing were excluded. The relative growth rate (RGR) was calculated (Massey & Hartley, 2009) as follows:

$$\text{RGR} = \frac{\text{Final mass} - \text{Initial mass}}{\text{Initial mass} \times \text{Time (days)}}$$

2.7.2 | Sample preparation

Larvae were gut-cleared by a 6 h food deprivation period (water provided) to minimise plant-derived carryover in homogenates, then snap-frozen and stored at −80°C. Two subsets of third-instar *H. armigera* larvae were used for biochemical analyses. For oxidative stress markers, phenoloxidase (PO) and energetic reserves, individual larvae ($n = 5$ per treatment) were homogenised in 600 μL ice-cold 0.1 M potassium phosphate buffer (pH 6.8) using a chilled bead-mill homogeniser. Homogenates were centrifuged at 15,000 × g for 10 min at 4°C, and the resulting supernatant was aliquoted for oxidative stress and PO assays. Energetic reserves were quantified using a sequential extraction approach modified from Foray et al. (2012). A separate subset of larvae ($n = 5$ per treatment) was used for antioxidant capacity and homogenised in 80% methanol for DPPH analysis. All aliquots were snap-frozen and stored at −80°C until analysis.

2.7.3 | Oxidative stress markers and antioxidant capacity

Hydrogen peroxide (H_2O_2) was quantified following Velikova et al. (2000). An aliquot of supernatant was mixed with 10 mM phosphate buffer (pH 7.0) and 1 M KI, and absorbance was read at 390 nm and expressed as μmol g^{-1} FW.

Malondialdehyde was measured using a TBARS assay (Sunkar et al., 2006). Aliquots were reacted with 0.5% TBA in 20% TCA, incubated at 95°C for 30 min, cooled, centrifuged and absorbance measured at 532 and 600 nm. Malondialdehyde equivalents were calculated using $\varepsilon = 155\,mM^{-1}\,cm^{-1}$ and expressed as μmol g^{-1} FW.

Phenoloxidase (PO) activity was assayed using L-DOPA as the substrate (Dularay & Lackie, 1985). Before analysis, PVPP (1% w/v) was added to the PO aliquot, gently mixed on ice and centrifuged

TABLE 1 Replication statement.

Scale of inference	Factor application scale	Replicates
Individual plant (*Triticum aestivum*)	UV-B (low/mod/high), Si (−/+), herbivory (−/+) applied at the plant level	$n=15$ per UV-B × Si × herbivory (total $n=180$); Si quantified on all replicates; $n=6$ per treatment for biochemical assays
Individual larva (*Helicoverpa armigera*)	Larvae assigned to plants from each UV-B × Si treatment	$n=12$–15 per UV-B × Si for RGR; $n=5$ per UV-B × Si for biochemical assays

Note: Scale of inference, the scale at which each factor was applied, and the number of replicates used in plant and insect analyses.

to obtain a clarified enzyme extract. For the assay, 25 μL of the supernatant was combined with 75 μL of 4 mg mL^{-1} L-DOPA and 100 μL phosphate buffer (pH 6.8) and incubated at 30°C for 5 min, and absorbance was measured at 490 nm.

Antioxidant capacity was quantified from methanolic extracts ($n=5$ per treatment) using the DPPH assay (Brand-Williams et al., 1995; Molyneux, 2004). Extract (100 μL) was mixed with 900 μL of 0.1 mM DPPH in methanol, incubated 30 min in darkness and absorbance recorded at 517 nm.

2.7.4 | Energetic resource quantification

Protein, soluble carbohydrates, lipids, triglycerides and glycogen were quantified following Foray et al. (2012). Protein content was quantified using the Bradford assay with bovine serum albumin as a standard. Absorbance was measured at 595 nm. Total carbohydrate content was assessed by mixing 100 μL of the supernatant with 900 μL of freshly prepared anthrone reagent (0.14% anthrone in 70% sulphuric acid). Samples were incubated at 90°C for 15 min and cooled on ice, and absorbance was measured at 625 nm with D-glucose as the standard. Glycogen content was measured from the methanol-washed pellet using the same anthrone procedure. Lipids and triglycerides were extracted from the supernatant using a 1:2 chloroform–methanol solution. Total lipids were quantified after sulphuric acid digestion followed by vanillin reagent reaction, with absorbance recorded at 525 nm. Triglycerides were isolated by binding polar lipids with silicic acid, and the neutral lipid fraction was quantified similarly using triolein as the standard. Energy reserve conversion was performed using standard energetic equivalents: 24,000 mJ mg^{-1} for protein, 39,500 mJ mg^{-1} for lipids and 17,500 mJ mg^{-1} for carbohydrates (Gnaiger, 1983; Masoumzadeh et al., 2017).

2.8 | Replication statement

2.8.1 | Statistical analysis

Plant and insect datasets were analysed separately. For plant traits, three-way ANOVA tested fixed effects of UV-B (low, moderate and high), Si (−Si, +Si) and herbivory (−H, +H), including all interaction terms (Table 1). For insect traits (measured only on herbivory plants), two-way ANOVA tested UV-B × Si (Table 1). Model assumptions (normality and homoscedasticity) were evaluated using residual diagnostics. H_2O_2 and MDA were log-transformed (ln), and RGR was transformed as ln(RGR + 1) prior to analysis to meet model assumptions. Significant main effects or interactions were followed by Tukey's HSD ($\alpha=0.05$).

Principal component analysis (PCA) was used to summarise covariation in (i) plant biochemical traits and (ii) insect physiological traits. Prior to ordination, variables were inspected for skew, log-transformed where appropriate, and then centred and scaled to unit variance (correlation matrix). PCA was conducted using replicate-level data; for clarity, figures show treatment centroids in ordination space (plants: UV-B × Si × herbivory; insects: UV-B × Si). To relate insect physiology to plant chemistry, we used redundancy analysis (RDA) with insect traits as responses and foliar Si (%) and total phenolics (mg GAE g^{-1} FW) as constraints; significance of constrained axes and terms was tested using 999 permutations.

Univariate analyses were conducted in Minitab (v21), and plotted in GraphPad Prism (v8.2.0; La Jolla, CA, USA). Multivariate analyses and ordination figures were generated in R (v4.5.1; R Core Team, 2025) using packages, including vegan (v2.7.1; Oksanen et al., 2025) and ggplot2 (v4.0.0; Wickham, 2016).

3 | RESULTS

3.1 | Plant responses

3.1.1 | Silicon accumulation

Foliar Si concentration was significantly increased by Si supplementation, with +Si plants accumulating 3.3-fold more Si than −Si plants (Figure 2; Table 2). Higher UV-B intensity reduced foliar Si: moderate and high UV-B were 8% lower than low UV-B, with no difference between moderate and high UV-B. Within +Si plants, foliar Si declined by 7–10% from low to moderate/high UV-B. Herbivory had no effect. −Si plants maintained consistently low background Si concentrations across all UV-B and herbivory treatments, with no significant effects of UV-B or herbivory (Table 2).

3.1.2 | Oxidative stress and antioxidant Defences

MDA was unaffected by UV-B alone, but consistently increased with herbivory, rising by 17.4% across treatments (Figure 3a; Table 2). A

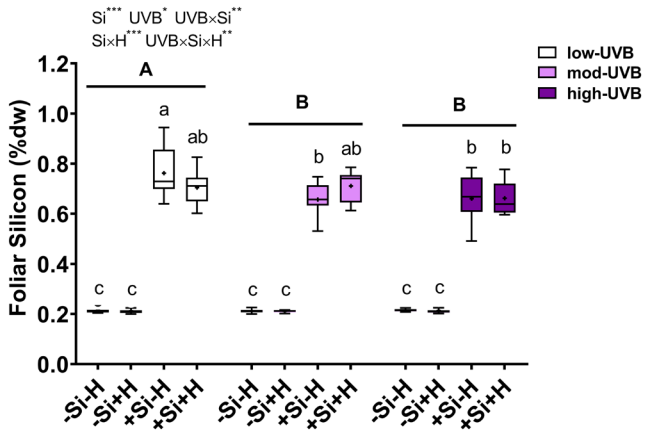

FIGURE 2 Foliar silicon concentration in wheat under silicon supplementation (+Si) and non-supplemented (−Si) conditions across ultraviolet-B (UV-B) intensities (low, moderate and high) with (+H) and without (−H) herbivory ($n = 10–15$ per UV-B × herbivory × Si combination). Crosses denote means. Different letters indicate significant differences (Tukey's HSD, $\alpha = 0.05$): Uppercase letters denote UV-B main effects and lowercase letters denote differences among treatment combinations. Asterisks indicate significant ANOVA terms (*$p < 0.05$, **$p < 0.01$, ***$p < 0.001$). Non-supplemented plants (−Si) reflect baseline foliar Si levels under Si-free hydroponic conditions.

significant UV-B × herbivory interaction showed that MDA peaked under moderate and high UV-B with herbivory. Silicon mitigated lipid peroxidation under low UV-B, where MDA remained comparable to control levels. A significant three-way interaction indicated that Si's protective effect was context-dependent and most evident under low UV-B.

H_2O_2 levels increased significantly with UV-B intensity, rising by 52% under high UV-B compared with low UV-B (Figure 3b; Table 2). Herbivory also elevated H_2O_2 concentrations by 13%, independent of UV-B or Si. Although Si had no significant main effect on H_2O_2, the highest levels were observed under the combined effect of high UV-B, herbivory and Si supplementation, resulting in a 67% increase relative to low UV-B controls.

Antioxidant capacity (DPPH) increased under moderate and high UV-B, with activity rising by 81% at high UV-B compared with low (Figure 3c; Table 2). Herbivory further increased antioxidant capacity by 53%. The highest antioxidant levels—up to 3.7-fold—were observed under high UV-B with herbivory, irrespective of Si. A significant Si × herbivory interaction showed that DPPH peaked in −Si plants under combined stress, while Si slightly reduced DPPH across treatments.

3.1.3 | Phenolics and defensive enzymes

Phenolic content and defence enzyme activity (PAL and PPO) varied significantly across treatments (Figure 4; Table 2). Phenolic concentrations increased significantly with UV-B, rising by 8% under moderate and 13% under high UV-B compared with low (Figure 4a; Table 2). Herbivory also elevated phenolics, but this response was strongly influenced by Si supply. A significant Si × herbivory interaction showed that herbivory-induced phenolics only in −Si plants, with levels rising by up to 30%. In contrast, Si supplementation significantly reduced phenolics with herbivory, with concentrations declining by 16.7% relative to −Si plants subject to herbivory. The strong three-way interaction showed that Si suppressed herbivory-induced phenolics by 21–25% under moderate UV-B and 14–18% under high UV-B (Figure 4a).

PAL activity was significantly influenced by all three main factors (Table 2). Moderate UV-B increased PAL by 16% compared with low UV-B, while high UV-B had no significant effect (Figure 4b; Table 2). Herbivory elevated PAL by 29%, and Si enhanced PAL under low UV-B but suppressed it under high UV-B. The highest PAL activity occurred in +Si, herbivore-treated plants under low UV-B—127% higher than the −Si, no-herbivory control. The three-way interaction was not significant (Figure 4b).

PPO activity rose with UV-B intensity, increasing by 29% under high compared with low UV-B (Figure 4c; Table 2). Herbivory triggered the strongest response, with PPO activity more than doubling in infested plants. Silicon increased PPO by 21% on average, especially under high UV-B without herbivory. PPO peaked under high UV-B with both herbivory and Si, reaching 2.7 times the level observed under low UV-B in −Si herbivore-free plants.

3.1.4 | Nutritional quality

Nitrogen-related traits followed similar patterns in terms of responses to Si supply, herbivory and UV-B. FAA and protein concentrations increased under high UV-B (by 33% and 9%, respectively) and with Si supplementation (by 25% and 16%, respectively) (Figure 5a,b; Table 2). Herbivory increased protein by 27% but had no effect on FAA. The highest levels of both traits were observed when all three factors co-occurred, with FAA and protein increasing by 82% and 97%, respectively. Conversely, the lowest values occurred under low UV-B in −Si herbivore-free plants.

Carbohydrate concentrations declined by 11% under high UV-B relative to low and moderate levels (Figure 5c; Table 2). Neither Si nor herbivory had main effects, but both partially offset UV-B-induced declines in specific combinations.

3.1.5 | Multivariate analysis of plant traits (PCA)

The plant PCA explained 50.83% of total variance across the first two axes (PC1 31.37%, PC2 19.46%; Figure 6). PC1 reflected the combined impact of UV-B exposure and herbivory: +H and high UV-B shifts plants towards the positive side of the ordination, consistent with coordinated increases in oxidative stress (MDA and H_2O_2) and a broader defence response (antioxidant capacity and defence-related enzymes), whereas −H plants under low UV-B clustered on the negative side, more closely associated with carbohydrate status. PC2 reflected the primary effect of Si

TABLE 2 Results of statistical analysis for silicon accumulation, oxidative status, phenolics-related defences and nutritional quality measurements in wheat plants as affected by ultraviolet-B (UV-B), Si supply, and herbivore presence and their interactive effects.

			UV-B		Silicon		Herbivory		UV-B × Si		UV-B × H		Si × H		UV-B × Si × H	
Plant response variables	**Figures**	**df**	***F***	***p***	***F***	***p***	***F***	***p***	***F***	***p***	***F***	***p***	***F***	***p***	***F***	***p***
Silicon accumulation																
Silicon (%)	2	167	6.74	**0.002****	3345.71	**0.0001*****	0.01	0.920	6.70	**0.002****	3.77	**0.025***	0.00	0.975	3.67	**0.028***
Oxidative status																
MDA	3a	60	2.52	0.089	10.07	**0.002*****	112.03	**0.0001*****	15.49	**0.0001*****	5.01	**0.010***	1.08	0.303	8.53	**0.001****
H_2O_2	3b	60	30.79	**0.0001*****	1.41	0.240	17.98	**0.0001*****	0.24	0.791	1.31	0.278	0.00	0.951	3.53	**0.036***
DPPH	3c	60	18.64	**0.0001*****	4.39	**0.040***	30.36	**0.0001*****	0.19	0.828	0.66	0.520	13.30	**0.001****	2.28	0.111
Phenolics-related defence																
Phenolics	4a	60	19.77	**0.0001*****	29.58	**0.0001*****	11.34	**0.001****	9.10	**0.0001*****	4.66	**0.013***	38.89	**0.0001*****	17.37	**0.0001*****
PAL	4b	60	5.62	**0.006*****	5.50	**0.022***	49.63	**0.0001*****	23.07	**0.0001*****	3.06	0.054	1.51	0.223	0.90	0.412
PPO	4c	60	6.96	**0.002*****	11.40	**0.001****	164.76	**0.000*****	3.45	**0.038***	0.62	0.539	0.59	0.446	4.85	**0.011***
Nutritional quality																
FAA	5a	60	16.27	**0.0001*****	29.21	**0.0001*****	0.61	0.437	6.53	**0.003****	0.16	0.850	1.02	0.316	3.14	0.051
Protein	5b	60	3.07	0.054	10.41	**0.002*****	27.10	**0.0001*****	4.83	**0.011***	1.13	0.330	2.61	0.111	12.63	**0.0001*****
Carb	5c	60	6.89	**0.002*****	0.73	0.396	1.16	0.285	3.38	**0.027***	4.01	**0.023***	0.01	0.936	0.98	0.382

Note: Factors with significant effects are indicated in bold with asterisks denoting levels of significance: $^{*}p < 0.05$, $^{**}p < 0.01$ and $^{***}p < 0.001$.

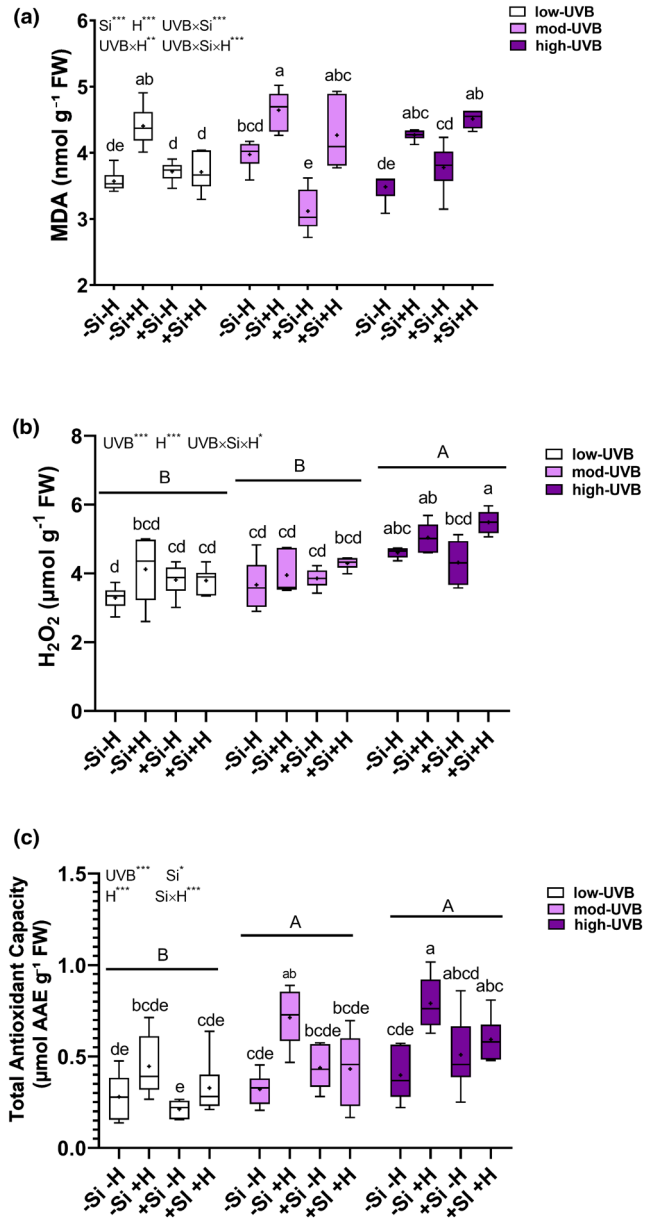

FIGURE 3 Foliar oxidative status and antioxidant capacity of wheat across ultraviolet-B (UV-B) intensity (low, moderate and high), silicon supplementation (−Si, +Si) and herbivory (−H, +H): (a) MDA, (b) H_2O_2, and (c) antioxidant capacity (DPPH). Crosses denote means ($n = 6$ per treatment). Different letters indicate significant differences (Tukey's HSD, $\alpha = 0.05$): Uppercase letters denote UV-B main effects and lowercase letters denote differences among treatment combinations. Asterisks indicate significant ANOVA terms (*$p < 0.05$, **$p < 0.01$, ***$p < 0.001$). H_2O_2 and MDA values are shown as ln-transformed data.

supplementation and revealed a clear trade-off between foliar Si and phenolics, with +Si treatments clustering at higher PC2 scores and − Si treatments at lower PC2 scores. Where +Si treatments were also positioned lower on PC1 than their −Si counterparts within comparable UV-B–herbivory combinations, this pattern was consistent with a reduced oxidative stress signature under Si supplementation (Figure 6).

3.2 | Insect responses

3.2.1 | Relative growth rate (RGR)

RGR was significantly reduced—by 35%—when insects fed on Si-supplemented wheat leaves, regardless of UV-B treatment (Figure 7; Table 3). No significant differences in RGR were detected among larvae feeding on plants grown under different UV-B levels.

3.2.2 | Oxidative stress and antioxidants

Larval oxidative stress and antioxidant responses varied depending on the UV-B exposure level of the host plants and Si availability (Figure 8; Table 3). H_2O_2 levels in larval tissues increased with UV-B intensity, reaching their maximum under high UV-B (Figure 8a). However, under all UV-B conditions, H_2O_2 was significantly lower—by 43% on average—in larvae feeding on Si-supplemented plants. Malondialdehyde concentrations peaked when larvae fed on plants exposed to high UV-B (36% higher) and low UV-B (25% higher) compared with moderate UV-B (Figure 8b). Larvae feeding on Si-supplemented plants exhibited consistently lower MDA concentrations.

DPPH activity was highest under moderate UV-B and declined with increasing UV-B intensity (Figure 8c). Antioxidant capacity was 1.2- to 5.7-fold higher in larvae fed on Si-supplemented plants, particularly under low and high UV-B.

PO activity followed a similar pattern, peaking under moderate UV-B (Figure 8d). Compared with this peak, activity declined by 33% and 53% when insects fed on plants exposed to low and high UV-B, respectively. Silicon supplementation increased PO by 56%, with the strongest effect observed under moderate UV-B.

3.2.3 | Energy reserves and metabolic adjustments

Larval energy reserves varied with both UV-B and Si treatment (Figure 9; Table 3). Carbohydrates declined by 52% under high UV-B relative to low UV-B (Figure 9a), but were 2.5-fold higher in Si-fed larvae under moderate UV-B. Glycogen showed the strongest Si response, reaching 2.9-fold higher levels in +Si larvae under high UV-B (Figure 9b). Lipid and triglyceride reserves declined progressively with UV-B intensity but were consistently higher in −Si larvae across all treatments, with lipids up to 2.6-fold higher under low UV-B in Si-free larvae (Figure 9c,d). Protein increased by 40% under high UV-B independent of Si (Figure 9e), and total energy equivalents showed no consistent treatment pattern (Figure 9f).

3.2.4 | Multivariate analysis of insect traits (PCA)

The insect PCA explained 62.97% of total variance across the first two axes (PC1 44.45%, PC2 18.52%; Figure 10). PC1 captured a primary

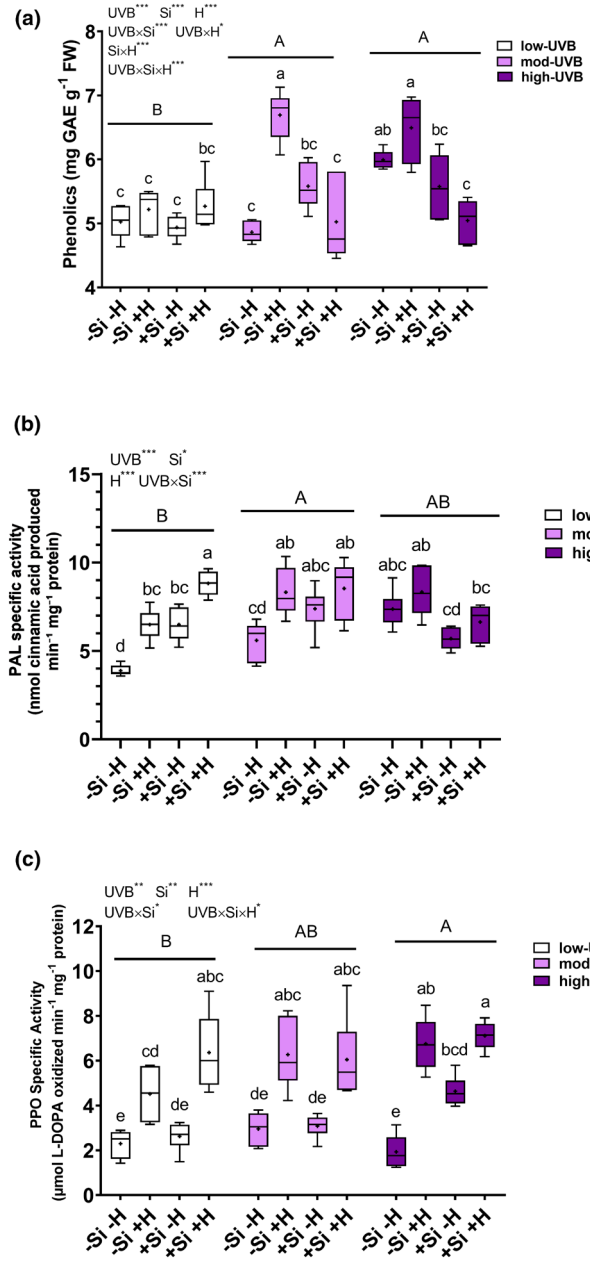

FIGURE 4 Phenolic-based defence responses in wheat across ultraviolet-B (UV-B) intensity (low, moderate and high), silicon supplementation (−Si, +Si) and herbivory (−H, +H). Panels show (a) total phenolics, (b) phenylalanine ammonia-lyase (PAL) specific activity and (c) polyphenol oxidase (PPO) specific activity. Crosses denote means ($n = 6$ per treatment). Different letters indicate significant differences (Tukey's HSD, $\alpha = 0.05$): Uppercase letters denote UV-B main effects and lowercase letters denote differences among treatment combinations. Asterisks indicate significant ANOVA terms (*$p < 0.05$, **$p < 0.01$, ***$p < 0.001$).

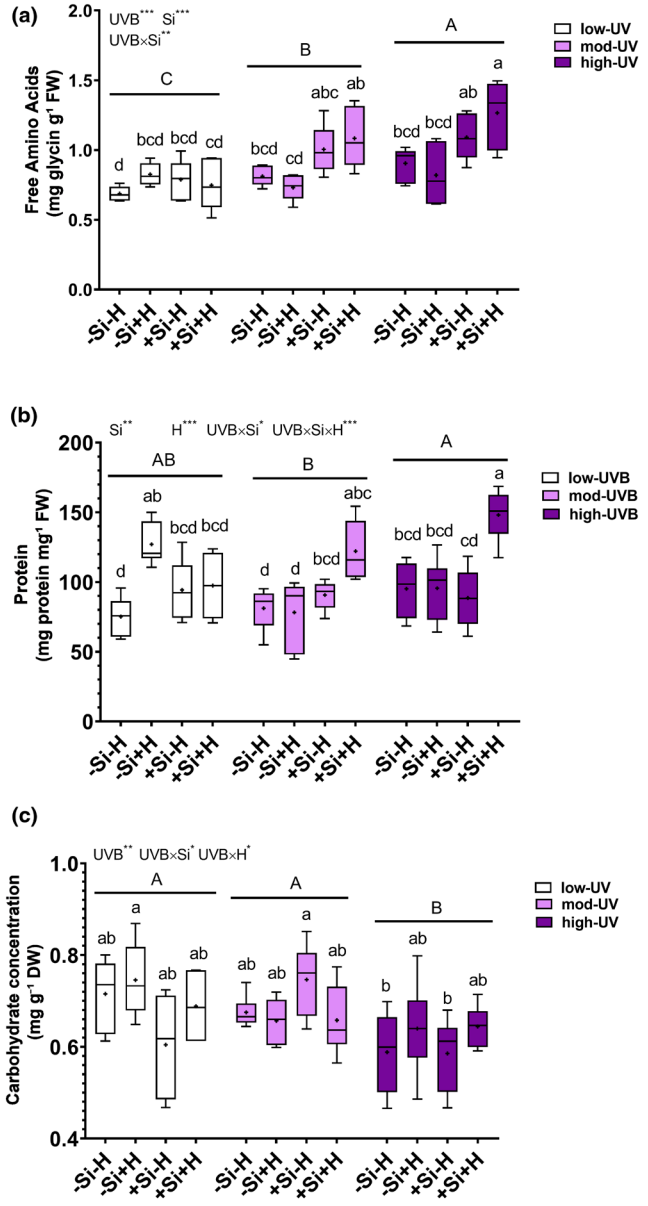

FIGURE 5 Nutritional quality in wheat across ultraviolet-B (UV-B) intensity (low, moderate, high), silicon supplementation (−Si, +Si) and herbivory (−H, +H). Panels show (a) free amino acids, (b) total protein and (c) carbohydrates. Crosses denote means ($n = 6$ per treatment). Different letters indicate significant differences (Tukey's HSD, $\alpha = 0.05$): Uppercase letters denote UV-B main effects and lowercase letters denote differences among treatment combinations. Asterisks indicate significant ANOVA terms (*$p < 0.05$, **$p < 0.01$, ***$p < 0.001$).

shift from larvae characterised by greater oxidative stress and poorer performance to those showing greater carbohydrate-based reserves and elevated PO activity. PC2 reflected metabolic allocation, separating individuals dominated by lipid-based energy storage from those positioned towards a more protein-associated trait profile. Treatment scores separated most strongly by Si along PC1: +Si larvae clustered towards the carbohydrate/glycogen and PO region, whereas −Si larvae aligned more closely with the oxidative stress and performance gradient. UV-B effects were expressed mainly as within-Si shifts along PC2, with high UV-B tending to shift −Si larvae towards the oxidative/protein direction relative to low/moderate UV-B, which were more associated with lipid-based reserves (Figure 10).

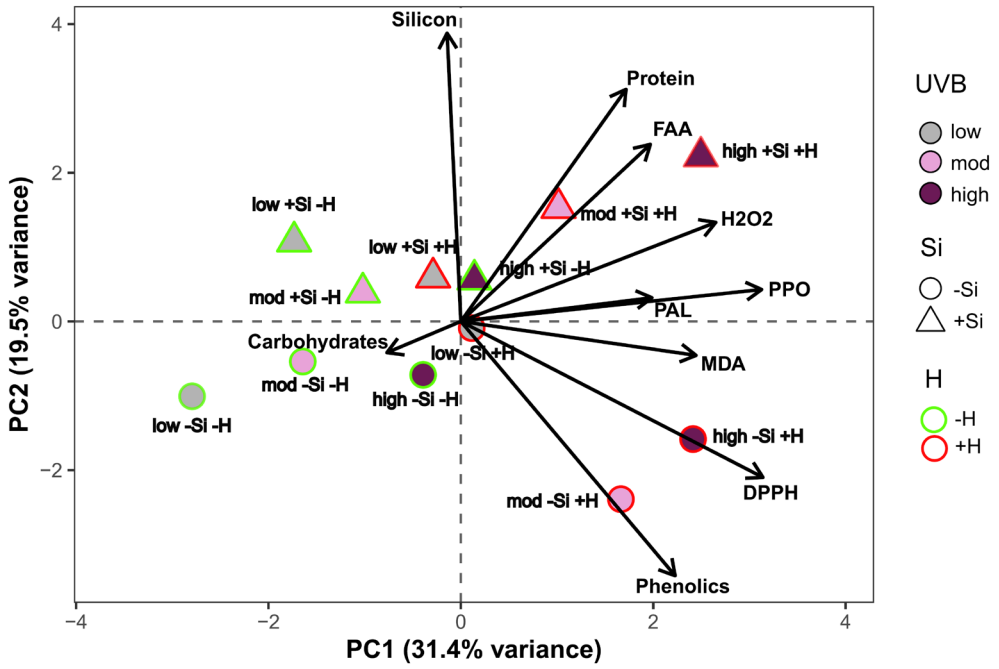

FIGURE 6 Principal component analysis (PCA) of plant biochemical traits under combined ultraviolet-B (UV-B) intensity (low, moderate and high), silicon supplementation (−Si, +Si) and herbivory (−H, +H). Arrows indicate trait loadings. Small symbols show individual replicates ($n = 6$ per treatment), and large symbols show treatment centroids. Colour denotes UV-B level, symbol shape denotes silicon treatment (circles = −Si; triangles = +Si), and symbol outline colours denote herbivory (Green: −H, Red: +H).

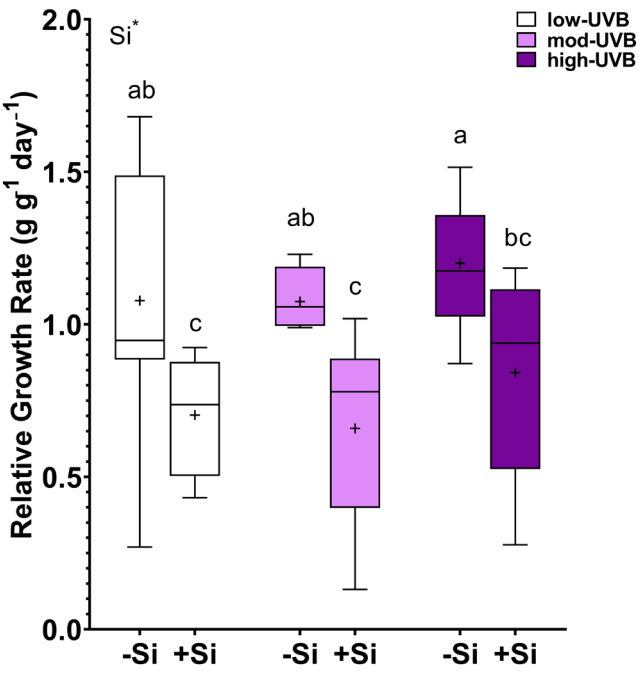

FIGURE 7 Relative growth rate (RGR) of *Helicoverpa armigera* larvae fed on wheat grown under ultraviolet-B (UV-B) intensity (low, moderate and high) and silicon supplementation (−Si, +Si). Crosses denote means ($n = 12$–15 per treatment). Different letters indicate significant differences (Tukey's HSD, $\alpha = 0.05$): Uppercase letters denote UV-B main effects and lowercase letters denote differences among treatment combinations. Asterisks indicate significant ANOVA terms (*$p < 0.05$, **$p < 0.01$, ***$p < 0.001$). Values are shown on the ln(RGR + 1) scale.

3.3 | Linking plant and insect responses (RDA)

RDA quantified how insect physiological variation was explained by foliar Si and total phenolics, with UV-B shown as treatment groupings (Figure 11). The constrained model explained 38.95% of total variance in insect traits (adjusted $R^2 = 0.344$). Variation explained was driven largely by plant Si (Variance = 3.7516, $F = 16.59$, $p = 0.001$), whereas phenolics did not contribute additional explanatory power once Si was included (Variance = 0.1436, $F = 0.64$, $p = 0.664$); collinearity was low (VIF = 1.91).

Constraint was concentrated on RDA1 (96.4% of constrained variance; $F = 16.60$, $p = 0.001$), while RDA2 explained 3.6% and was not supported ($F = 0.63$, $p = 0.722$). Along RDA1, higher foliar Si aligned with larval profiles characterised by higher carbohydrate/glycogen reserves and PO activity, whereas lower Si aligned with higher oxidative stress (MDA, H_2O_2) and a shift towards lipid/triglyceride-associated allocation (Figure 11).

4 | DISCUSSION

Interactions between UV-B radiation, herbivory and Si supplementation determined the allocation of wheat defences with cascading impacts on *Helicoverpa armigera*. UV-B reduced foliar Si while increasing oxidative signalling (H_2O_2) and antioxidant activity (DPPH). Herbivory further elevated lipid peroxidation (MDA) and defence enzyme activities (PAL and PPO). Si acted as a conditional modulator of wheat oxidative response, most effective under moderate UV-B and without

TABLE 3 Results of statistical analysis for relative growth rate, oxidative status and energy reserves measurements in *H. armigera* larvae as affected by ultraviolet-B (UV-B) and Si supply and their interactive effects.

			UV-B		Silicon		UV-B × Si	
Insect responses variable	**Figures**	**df**	***F***	***p***	***F***	***p***	***F***	***p***
Insect performance								
RGR	7	68	2.02	0.141	32.08	**0.0001*****	0.06	0.938
Oxidative status								
H_2O_2	8a	24	22.76	**0.0001*****	84.45	**0.0001*****	17.19	**0.0001*****
MDA	8b	24	17.39	**0.0001*****	382.25	**0.0001*****	11.87	**0.0001*****
DPPH	8c	24	59.88	**0.0001*****	82.79	**0.0001*****	13.42	**0.0001*****
PO	8d	24	39.29	**0.0001*****	38.89	**0.0001*****	5.05	**0.015***
Energy reserves								
Carb	9a	24	13.22	**0.0001*****	23.31	**0.0001*****	3.89	**0.034***
Glycogen	9b	24	1.07	0.358	60.49	**0.0001*****	14.15	**0.0001*****
Lipid	9c	24	3.82	**0.036***	33.09	**0.0001*****	6.37	**0.006****
Triglyceride	9d	24	11.94	**0.0001*****	26.20	**0.0001*****	7.06	**0.004****
Protein	9e	24	5.23	**0.013***	1.26	0.273	0.15	0.860
Energy equivalent	9f	24	0.23	0.794	50.83	0.371	9.03	**0.001****

Note: Factors with significant effects are indicated in bold with asterisks denoting levels of significance: $^{*}p<0.05$, $^{**}p<0.01$ and $^{***}p<0.001$.

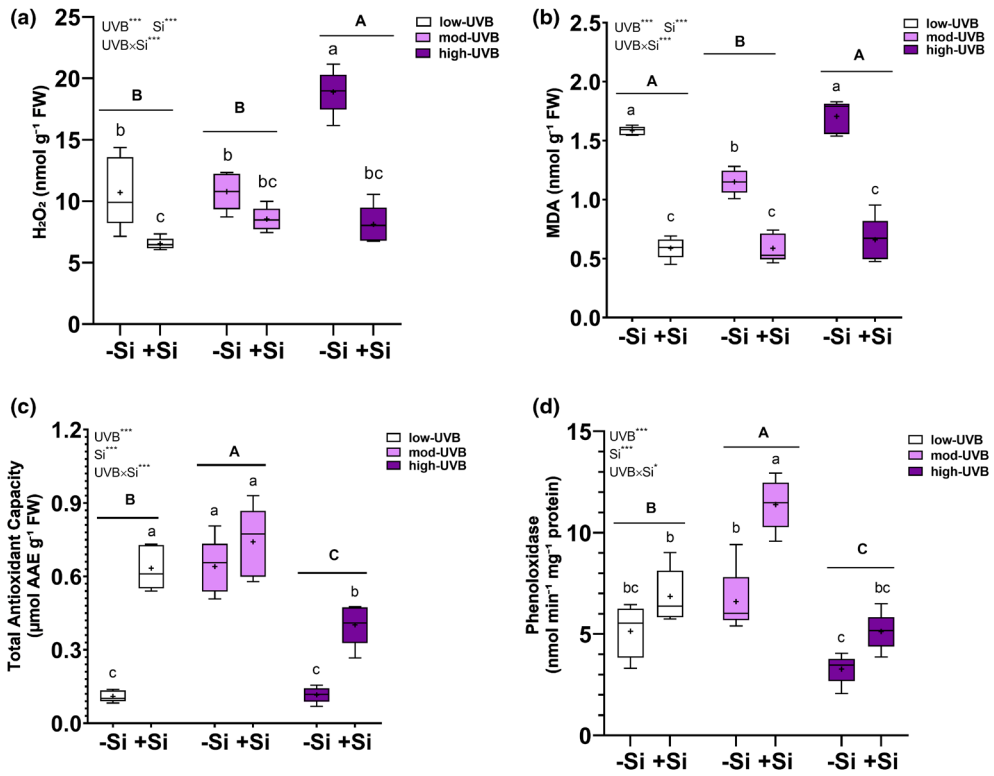

FIGURE 8 Antioxidative responses in *Helicoverpa armigera* larvae fed on wheat previously exposed to ultraviolet-B (UV-B) intensity (low, moderate and high) and silicon supplementation (−Si, +Si). Panels show (a) hydrogen peroxide (H_2O_2), (b) malondialdehyde (MDA), (c) DPPH antioxidant capacity and (d) phenoloxidase (PO) activity. Crosses denote means ($n=5$ per treatment). Different letters indicate significant differences (Tukey's HSD, $\alpha=0.05$): Uppercase letters denote UV-B main effects and lowercase letters denote differences among treatment combinations. Asterisks indicate significant ANOVA terms ($^{*}p<0.05$, $^{**}p<0.01$, $^{***}p<0.001$).

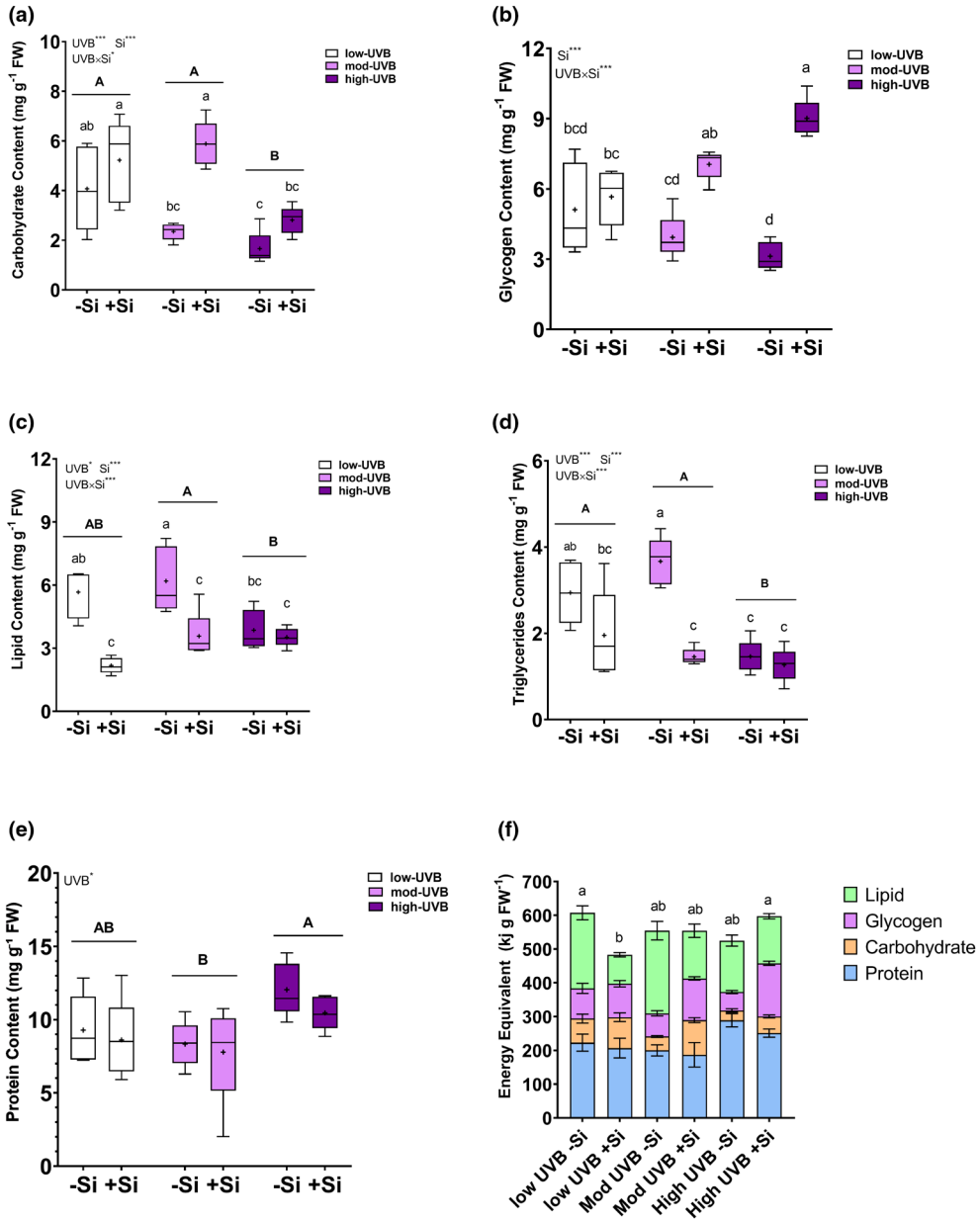

FIGURE 9 Energy-storage traits in *Helicoverpa armigera* larvae fed on wheat previously exposed to ultraviolet-B (UV-B) intensity (low, moderate and high) and silicon supplementation (−Si, +Si). Panels show (a) carbohydrates, (b) glycogen, (c) lipids, (d) triglycerides, (e) protein and (f) total energy equivalents. Crosses denote means ($n = 5$ per treatment). Different letters indicate significant differences (Tukey's HSD, $\alpha = 0.05$): Uppercase letters denote UV-B main effects and lowercase letters denote differences among treatment combinations. Asterisks indicate significant ANOVA terms (*$p < 0.05$, **$p < 0.01$, ***$p < 0.001$).

herbivory, alleviating oxidative damage and altering metabolic/defence allocation. In contrast, Si supplementation consistently reduced *H. armigera* growth across all UV-B intensities, despite UV-B constraints on foliar Si accumulation. Larvae feeding on Si-supplemented plants showed consistently reduced growth (RGR), lowered oxidative stress markers and shifts towards glycogen- and carbohydrate-based reserves. Multivariate analyses confirmed tight coupling between plant defence chemistry and insect redox/metabolic responses, highlighting that Si plays a crucial role in mediating UV-B-driven multitrophic interactions. Overall, our findings support H_1 (UV-B elevates oxidative signalling and defence induction) and H_4 (plant responses cascade to herbivore growth, redox physiology and energy allocation) and provide context-dependent support for H_2 (Si buffers oxidative damage and shifts defence investment) and H_3 (UV-B×herbivory effects depend on Si supply), as detailed below.

4.1 | Silicon buffers UV-B- and herbivory-induced oxidative stress

UV-B exposure increased H_2O_2, DPPH and PPO, but not MDA. This pattern aligns with H_1, indicating UV-B primarily elevates oxidative

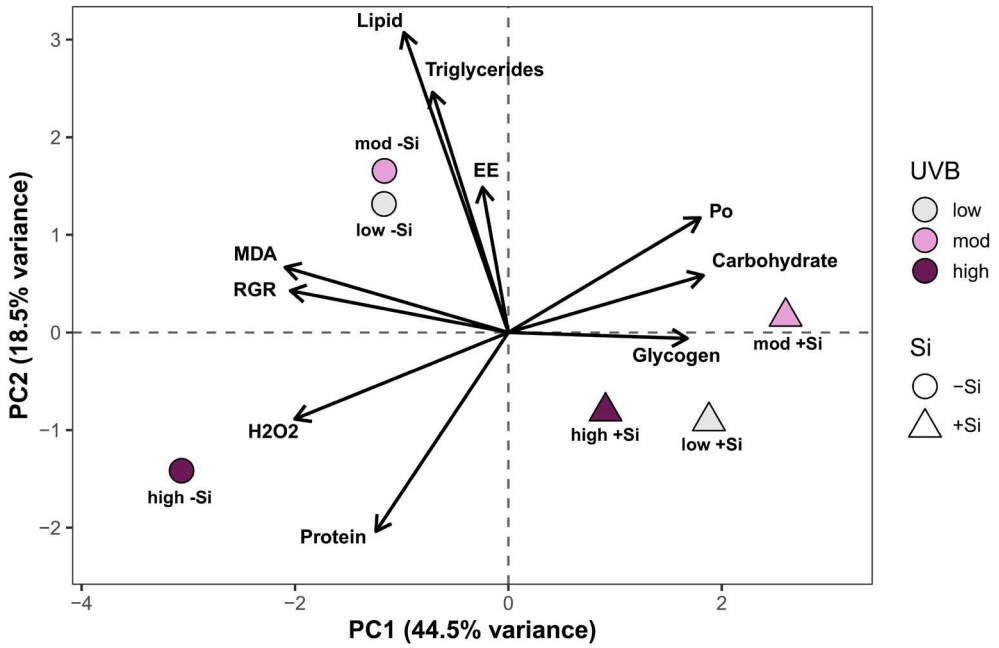

FIGURE 10 Principal component analysis (PCA) of *Helicoverpa armigera* physiological traits for larvae reared on wheat previously exposed to ultraviolet-B (UV-B) intensity (low, moderate and high) with or without silicon supplementation (−Si, +Si). Arrows indicate trait loading vectors. Small symbols represent biological replicates ($n = 5$ per treatment), and large symbols represent treatment centroids. Colour denotes UV-B level and symbol shape denotes silicon treatment (circles = −Si; triangles = +Si). PC1 and PC2 explain 44.5% and 18.5% of the total variance, respectively.

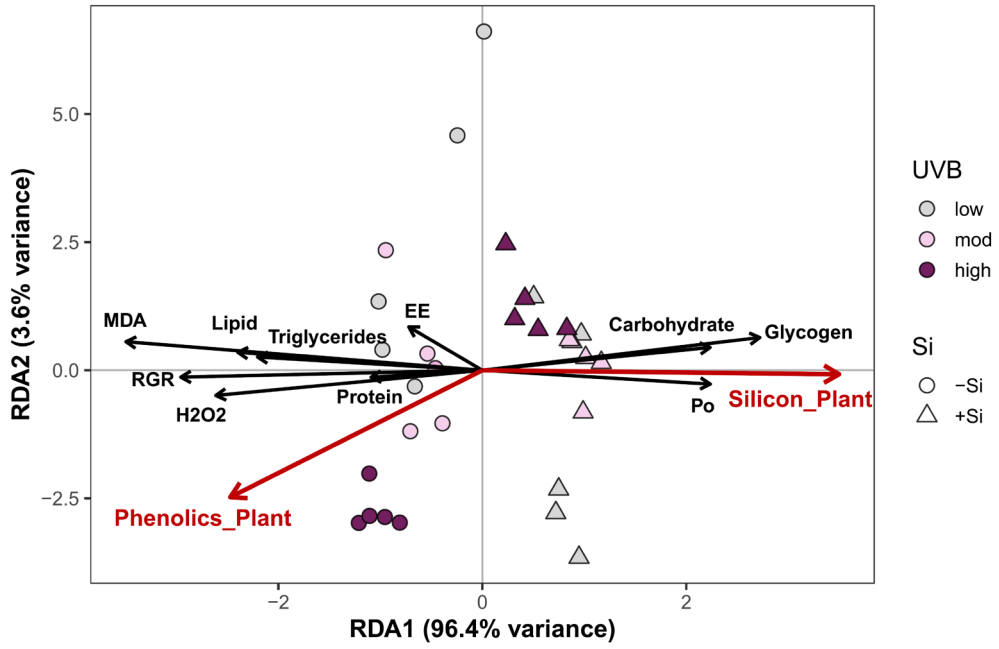

FIGURE 11 Redundancy analysis (RDA) relating *Helicoverpa armigera* physiological traits (black vectors) to plant chemical constraints (red vectors: foliar silicon and phenolics) across ultraviolet-B (UV-B) intensity (low, moderate and high) and silicon supplementation (−Si, +Si). Vector direction and length indicate the strength and sign of associations with the ordination axes. Points represent biological replicates ($n = 5$ per treatment), coloured by UV-B level and shaped by Si treatment. Axis percentages indicate the proportion of constrained variance explained. The constrained model explained 38.95% of total variance in insect traits (adjusted $R^2 = 0.344$; 999 permutations).

signalling and induces compensatory antioxidant responses rather than pervasive membrane damage. Plants likely acclimated to 5 weeks of UV-B exposure (up to 1.15 W/m^2; 20.7 $kJ\,m^{-2}\,d^{-1}$), levels within natural field ranges and lower than in some Si–UV-B studies (Malčovská et al., 2014; Shen, Li, et al., 2010; Shen, Zhou, et al., 2010). Si reduced MDA under moderate UV-B and partly under combined UV-B and herbivory, consistent with Si's known role in ROS detoxification and membrane stability (Shen, Zhou, et al., 2010; Tripathi et al., 2017; Yao et al., 2011) and in line with H_2 (Si buffers oxidative damage). This protective effect likely reflects Si-mediated enhancement of antioxidant capacity, evidenced by elevated radical scavenging (DPPH) and increased PPO activity, limiting oxidative damage despite elevated oxidative signalling. At higher UV-B, Si was less effective, suggesting a context-dependent threshold in its protective capacity. Under these conditions, elevated H_2O_2 may function primarily as a signalling molecule that triggers downstream acclimatory and defensive pathways, rather than serving as a direct indicator of oxidative damage (Saxena et al., 2016). This shift from damage mitigation towards signalling coordination likely contributes to Si-mediated rebalancing of defence allocation under combined stress, consistent with H_3 that UV-B and herbivory effects on oxidative outcomes are conditional on Si supply.

4.2 | Silicon shifts Defence allocation away from phenolic accumulation under UV-B and herbivory

Reduced phenolic content under Si supplementation, particularly under high UV-B and herbivory, supported the predicted shift away from phenolic investment (H_2). This represents a resource allocation trade-off in which Si-based investment can partially substitute for carbon-based phenylpropanoid defences, as previously documented under herbivory and elevated CO_2 (Cooke & Leishman, 2012; Fauteux et al., 2006; Frew et al., 2016) and under UV-B stress (Malčovská et al., 2014). Herbivory did not induce additional Si accumulation at the whole-canopy level, consistent with evidence that damage-induced Si responses in wheat are localised to damaged tissue rather than systemic (Thorne et al., 2023), and that a threshold level of damage is required for detectable induction (Hartley & DeGabriel, 2016)—which a single larva over 7 days may not have achieved. Here, multivariate analyses confirmed a trade-off between phenolic- and Si-associated defence strategies, with supplementation maintaining foliar Si even under high UV-B. Although PAL activity was enhanced by UV-B and herbivory, particularly in Si-free plants, this did not translate into increased phenolic accumulation in Si-treated plants. Instead, elevated PPO activity in Si-treated plants indicates a compensatory shift away from phenolic accumulation towards phenol oxidation–based defence pathways. This accelerated conversion of phenolics into reactive products can reduce foliage nutritive value and contribute to resistance against chewing herbivores (Barbehenn et al., 2005; Singh et al., 2020). Critically, Si supplementation suppressed *H. armigera* growth even when UV-B constrained foliar Si accumulation, indicating that resistance reflected coordinated defence expression rather than foliar Si alone, consistent with H_2 and H_3.

4.3 | Silicon suppresses larval growth across UV-B, while UV-B–Induced Plant chemistry elevates larval oxidative stress

Consistent with H_4 (plant responses cascade to herbivore growth and physiology), Si supplementation consistently reduced larval growth across all UV-B treatments, indicating that Si-based resistance remained effective even when environmental conditions constrained Si accumulation. This mirrors evidence across drought, elevated CO_2 and warming, indicating that Si-induced resistance is broadly consistent in imposing mechanical and nutritional constraints on herbivores (Hall et al., 2020; Johnson & Hartley, 2018; Vandegeer et al., 2021). Notably, UV-B alone did not impair RGR, suggesting *H. armigera*'s high detoxification capacity and dietary plasticity (Barbehenn, 2001; S. Chen et al., 2019; Mao et al., 2007) contrasts with more UV-B-sensitive lepidopterans (Izaguirre et al., 2007; Rousseaux et al., 2004). However, larval oxidative stress increased with plant UV-B exposure, likely reflecting the ingestion of UV-B-induced phenolics that act as pro-oxidants, with the magnitude of this effect depending on Si supply. Such compounds can deplete gut antioxidant pools and elevate redox cycling, amplifying endogenous oxidative load (Punia & Chauhan, 2022; Summers & Felton, 1994). In parallel, Si supplementation imposed a dual chemical–physical cost on larvae (Hall et al., 2019). Si induced an increase in plant PPO activity, likely enhancing phenol oxidation and the production of reactive quinones that impose an immediate oxidative cost on larvae. Physically, Si-driven structural resistance accelerates mandibular wear, generating a longer-term physical cost that further limits feeding efficiency (Massey & Hartley, 2009).

Despite the oxidative challenges, larval antioxidant responses varied with UV-B intensity. Antioxidant responses peaked under moderate UV-B but declined under high UV-B, suggesting a physiological threshold beyond which larval antioxidant and detoxification pathways became saturated, limiting their ability to counteract increasing oxidative load (Karthi et al., 2014). UV-B-stressed plants likely offered fewer dietary antioxidants (Mewis et al., 2012; Xu et al., 2008), compounding larval oxidative stress in the intestine. Notably, Si paradoxically mitigated larval oxidative markers (lower H_2O_2 and MDA). This pattern likely reflects stress avoidance driven by reduced feeding and altered digestibility imposed by Si-based physical resistance, which limits larval exposure to redox-active phytochemicals. Additionally, Si-mediated reductions in foliar oxidative damage may have reduced the oxidative load of ingested plant tissue, contributing to lower larval H_2O_2 and MDA. Elevated PO activity in Si-fed larvae suggests compensatory enzymatic detoxification; however, the overall reduction in oxidative damage indicators supports feeding deterrence rather than enhanced physiological resilience. Consistent with this pathway, RDA identified plant Si and phenolics as significant predictors of larval redox variation, linking oxidative physiology directly to plant defence chemistry as predicted by H_4.

4.4 | Plant-mediated stress shifts larval energy allocation from lipid storage towards immediate carbohydrate use

Feeding on plants exposed to high UV-B shifted larval energy allocation away from storage: carbohydrate, lipid and triglyceride pools were depleted, while protein pools increased and there was no consistent trend in total energy equivalents (sum of quantified reserve pools converted to energy units). These metabolic shifts align with H_4, reflecting reserve mobilisation and elevated maintenance costs under stress (Arrese & Soulages, 2010; Villena et al., 2018) and with greater investment in protein-based stress response, particularly antioxidant and detoxification systems, expected under a more pro-oxidant host diet (Dong et al., 2024; Karthi et al., 2014; Yang et al., 2022). Larvae feeding on Si-supplemented plants, particularly under moderate UV-B, shifted energy reserves towards readily mobilisable carbohydrates and glycogen, indicating reallocation of resources to meet immediate metabolic demands imposed by feeding inhibition and oxidative stress. In contrast, Si-free larvae on low UV-B accumulated lipids and triglycerides, investing in long-term reserves for supporting reproduction and dispersal (Arrese & Soulages, 2010; Foray et al., 2012; Toprak et al., 2020). Despite these reallocations, growth remained suppressed on Si-supplemented plants, highlighting the combined cost of reduced digestibility and mandibular wear (Massey & Hartley, 2009; Moise et al., 2019) and reinforcing the cascading effects on herbivore energy allocation anticipated under H_4.

5 | CONCLUSION

Global climate change is expected to increase the overlap between high UV-B exposure and herbivory pressure in many ecosystems, making it essential to understand how crops rebalance defence portfolios across interacting biotic and abiotic environmental drivers rather than under a single driver. Using a fully factorial test of Si supply × UV-B intensity × herbivory in a wheat–herbivore system, with an ecologically realistic UV-B gradient, we show that UV-B constrains foliar Si accumulation, yet Si supplementation maintains resistance against *H. armigera*, consistent with a shift from carbon-based phenolic investment towards Si-based protection. This defence reallocation cascades to herbivores, altering larval redox physiology and energy allocation towards readily mobilisable carbohydrate reserves. These findings support H_1–H_4, with particularly strong evidence for UV-B-driven oxidative signalling (H_1), multitrophic cascading effects (H_4), and context-dependent Si buffering of oxidative damage under combined UV-B and herbivory stress (H_2, H_3). This context dependence demonstrates the value of incorporating Si-based defence into forecasting frameworks for crop vulnerability and pest pressure in an ongoing changing climate. More broadly, natural gradients of UV-B exposure and silicon availability may play an underappreciated role in modulating Si-C defence trade-offs in Si-accumulating grasses across grasslands and agroecosystems.

AUTHOR CONTRIBUTIONS

Sajjad Reyhani Haghighi: Conceptualisation (lead); methodology (lead); investigation (lead); data curation (lead); data analysis (lead); visualisation (lead); writing—original draft (lead). **Scott N. Johnson:** Conceptualisation (equal); methodology (supporting); supervision (lead); project administration (supporting); funding acquisition (supporting); validation (lead); writing—review and editing (equal). **Christopher I. Cazzonelli:** Supervision (equal); resources (supporting); writing—review and editing (equal). **Sue E. Hartley:** supervision (equal); writing—review and editing (equal).

ACKNOWLEDGEMENTS

We thank Farzana Nowrin, Ramalka Kasige, Xuqing Li and Amir Tourani for assistance with herbivore infestations and insect collection. We also thank Andrew Gherlenda and Burhan Amiji for technical support with the UV-B lamp setup, and Sachin Chavan for training and support with the PS-300 spectroradiometer. This research was supported by the Commonwealth through an Australian Government Research Training Program Scholarship [DOI: https://doi.org/10.82133/C42F-K220]. Open access publishing facilitated by Western Sydney University, as part of the Wiley - Western Sydney University agreement via the Council of Australasian University Librarians

CONFLICT OF INTEREST STATEMENT

The authors declare that there is no conflict of interest.

DATA AVAILABILITY STATEMENT

Data are available from figshare: https://doi.org/10.6084/m9.figshare.31368490 (Reyhani-Haghighi et al., 2026).

ORCID

Sajjad Reyhani Haghighi https://orcid.org/0000-0001-9485-7088
Sue E. Hartley https://orcid.org/0000-0002-5117-687X
Scott N. Johnson https://orcid.org/0000-0002-8388-8345

REFERENCES

Ainsworth, E. A., & Gillespie, K. M. (2007). Estimation of total phenolic content and other oxidation substrates in plant tissues using Folin–Ciocalteu reagent. *Nature Protocols*, *2*(4), 875–877. https://doi.org/10.1038/nprot.2007.102

Arrese, E. L., & Soulages, J. L. (2010). Insect fat body: Energy, metabolism, and regulation. *Annual Review of Entomology*, *55*, 207–225. https://doi.org/10.1146/annurev-ento-112408-085356

Barbehenn, R., Cheek, S., Gasperut, A., Lister, E., & Maben, R. (2005). Phenolic compounds in red oak and sugar maple leaves have pro-oxidant activities in the midgut fluids of *Malacosoma disstria* and *Orgyia leucostigma* caterpillars. *Journal of Chemical Ecology*, *31*(5), 969–988. https://doi.org/10.1007/s10886-005-4242-4

Barbehenn, R. V. (2001). Roles of peritrophic membranes in protecting herbivorous insects from ingested plant allelochemicals. *Archives of Insect Biochemistry and Physiology*, *47*(2), 86–99. https://doi.org/10.1002/arch.1039

Barbehenn, R. V., Maben, R. E., & Knoester, J. J. (2008). Linking phenolic oxidation in the midgut lumen with oxidative stress in the midgut tissues of a tree-feeding caterpillar *Malacosoma disstria*

(lepidoptera: Lasiocampidae). *Environmental Entomology*, *37*(5), 1113–1118. https://doi.org/10.1603/0046-225x(2008)37[1113:lpoitm]2.0.co;2

Biru, F. N., Islam, T., Cibils-Stewart, X., Cazzonelli, C. I., Elbaum, R., & Johnson, S. N. (2021). Anti-herbivore silicon defences in a model grass are greatest under Miocene levels of atmospheric CO2. *Global Change Biology*, *27*(12), 2959–2969. https://doi.org/10.1111/gcb.15619

Bradford, M. M. (1976). A rapid and sensitive method for the quantitation of microgram quantities of protein utilizing the principle of protein-dye binding. *Analytical Biochemistry*, *72*(1), 248–254. https://doi.org/10.1016/0003-2697(76)90527-3

Brand-Williams, W., Cuvelier, M. E., & Berset, C. (1995). Use of a free radical method to evaluate antioxidant activity. *LWT - Food Science and Technology*, *28*(1), 25–30. https://doi.org/10.1016/S0023-6438(95)80008-5

Chen, S., Elzaki, M. E. A., Ding, C., Li, Z., Wang, J., Zeng, R., & Song, Y.-Y. (2019). Plant allelochemicals affect tolerance of polyphagous lepidopteran pest *Helicoverpa armigera* (Hübner) against insecticides. *Pesticide Biochemistry and Physiology*, *154*, 32–38. https://doi.org/10.1016/j.pestbp.2018.12.009

Chen, Z., Dong, Y., & Huang, X. (2022). Plant responses to UV-B radiation: Signaling, acclimation and stress tolerance. *Stress Biology*, *2*(1), 51. https://doi.org/10.1007/s44154-022-00076-9

Cooke, J., & Leishman, M. R. (2012). Tradeoffs between foliar silicon and carbon-based defences: Evidence from vegetation communities of contrasting soil types. *Oikos*, *121*(12), 2052–2060. https://doi.org/10.1111/j.1600-0706.2012.20057.x

Correia, C. M., Coutinho, J. F., Björn, L. O., & Torres-Pereira, J. M. G. (2000). Ultraviolet-B radiation and nitrogen effects on growth and yield of maize under Mediterranean field conditions. *European Journal of Agronomy*, *12*(2), 117–125. https://doi.org/10.1016/S1161-0301(99)00050-7

Demkura, P. V., Abdala, G., Baldwin, I. T., & Ballaré, C. L. (2010). Jasmonate-dependent and -independent pathways mediate specific effects of solar ultraviolet B radiation on leaf phenolics and antiherbivore defense. *Plant Physiology*, *152*(2), 1084–1095. https://doi.org/10.1104/pp.109.148999

Dong, W., Hou, D., Hou, Q., Jin, H., Li, F., & Wu, S. (2024). Effects of ultraviolet light stress on protective and detoxification enzymes in insects. *Tropical Plants*, *3*(1), e007. https://doi.org/10.48130/tp-0024-0008

Duckworth, H. W., & Coleman, J. E. (1970). Physicochemical and kinetic properties of mushroom tyrosinase. *Journal of Biological Chemistry*, *245*(7), 1613–1625. https://doi.org/10.1016/S0021-9258(19)77137-3

Dularay, B., & Lackie, A. M. (1985). Haemocytic encapsulation and the prophenoloxidase-activation pathway in the locust *Schistocerca gregaria* forsk. *Insect Biochemistry*, *15*(6), 827–834. https://doi.org/10.1016/0020-1790(85)90112-X

Escobar-Bravo, R., Nederpel, C., Naranjo, S., Kim, H. K., Rodríguez-López, M. J., Chen, G., Glauser, G., Leiss, K. A., & Klinkhamer, P. G. L. (2021). Ultraviolet radiation modulates both constitutive and inducible plant defenses against thrips but is dose and plant genotype dependent. *Journal of Pest Science*, *94*(1), 69–81. https://doi.org/10.1007/s10340-019-01166-w

Fauteux, F., Chain, F., Belzile, F., Menzies, J. G., & Bélanger, R. R. (2006). The protective role of silicon in the Arabidopsis–powdery mildew pathosystem. *Proceedings of the National Academy of Sciences*, *103*(46), 17554–17559. https://doi.org/10.1073/pnas.0606330103

Flint, S. D., & Caldwell, M. M. (2003). A biological spectral weighting function for ozone depletion research with higher plants. *Physiologia Plantarum*, *117*(1), 137–144. https://doi.org/10.1034/j.1399-3054.2003.1170117.x

Foray, V., Pelisson, P.-F., Bel-Venner, M.-C., Desouhant, E., Venner, S., Menu, F., Giron, D., & Rey, B. (2012). A handbook for uncovering the complete energetic budget in insects: The van Handel's method (1985) revisited. *Physiological Entomology*, *37*(3), 295–302. https://doi.org/10.1111/j.1365-3032.2012.00831.x

Frew, A., Powell, J. R., Sallam, N., Allsopp, P. G., & Johnson, S. N. (2016). Trade-offs between silicon and phenolic defenses may explain enhanced performance of root herbivores on phenolic-rich plants. *Journal of Chemical Ecology*, *42*(8), 768–771. https://doi.org/10.1007/s10886-016-0734-7

Gnaiger, E. (1983). Calculation of energetic and biochemical equivalents of respiratory oxygen consumption. In E. Gnaiger & H. Forstner (Eds.), *Polarographic oxygen sensors* (pp. 337–345). Springer. https://doi.org/10.1007/978-3-642-81863-9_30

Goto, M., Ehara, H., Karita, S., Takabe, K., Ogawa, N., Yamada, Y., Ogawa, S., Yahaya, M. S., & Morita, O. (2003). Protective effect of silicon on phenolic biosynthesis and ultraviolet spectral stress in rice crop. *Plant Science*, *164*(3), 3. https://doi.org/10.1016/S0168-9452(02)00419-3

Hall, C. R., Mikhael, M., Hartley, S. E., & Johnson, S. N. (2020). Elevated atmospheric CO2 suppresses jasmonate and silicon-based defences without affecting herbivores. *Functional Ecology*, *34*(5), 993–1002. https://doi.org/10.1111/1365-2435.13549

Hall, C. R., Waterman, J. M., Vandegeer, R. K., Hartley, S. E., & Johnson, S. N. (2019). The role of silicon in antiherbivore phytohormonal Signalling. *Frontiers in Plant Science*, *10*, 1132. https://doi.org/10.3389/fpls.2019.01132

Hamann, E., Blevins, C., Franks, S. J., Jameel, M. I., & Anderson, J. T. (2021). Climate change alters plant–herbivore interactions. *New Phytologist*, *229*(4), 1894–1910. https://doi.org/10.1111/nph.17036

Hartley, S. E., & DeGabriel, J. L. (2016). The ecology of herbivore-induced silicon defences in grasses. *Functional Ecology*, *30*(8), 1311–1322. https://doi.org/10.1111/1365-2435.12706

Hideg, E., Jansen, M. A. K., & Strid, A. (2013). UV-B exposure, ROS, and stress: Inseparable companions or loosely linked associates? *Trends in Plant Science*, *18*(2), 107–115. https://doi.org/10.1016/j.tplants.2012.09.003

Islam, T., Moore, B. D., & Johnson, S. N. (2023). Silicon fertilisation affects morphological and immune defences of an insect pest and enhances plant compensatory growth. *Journal of Pest Science*, *96*(1), 41–53. https://doi.org/10.1007/s10340-022-01478-4

Izaguirre, M. M., Mazza, C. A., SvatoŠ, A., Baldwin, I. T., & BallarÉ, C. L. (2007). Solar ultraviolet-B radiation and insect herbivory trigger partially overlapping phenolic responses in *Nicotiana attenuata* and *Nicotiana longiflora*. *Annals of Botany*, *99*(1), 103–109. https://doi.org/10.1093/aob/mcl226

Johnson, S. N., & Hartley, S. E. (2018). Elevated carbon dioxide and warming impact silicon and phenolic-based defences differently in native and exotic grasses. *Global Change Biology*, *24*(9), 3886–3896. https://doi.org/10.1111/gcb.13971

Karthi, S., Sankari, R., & Shivakumar, M. S. (2014). Ultraviolet-B light induced oxidative stress: Effects on antioxidant response of *Spodoptera litura*. *Journal of Photochemistry and Photobiology B: Biology*, *135*, 1–6. https://doi.org/10.1016/j.jphotobiol.2014.04.008

Kriticos, D. J., Ota, N., Hutchison, W. D., Beddow, J., Walsh, T., Tay, W. T., Borchert, D. M., Paula-Moreas, S. V., Czepak, C., & Zalucki, M. P. (2015). The potential distribution of invading Helicoverpa armigera in North America: Is it just a matter of time? *PLoS One*, *10*(3), e0119618. https://doi.org/10.1371/journal.pone.0119618

Lalouette, L., Williams, C. M., Hervant, F., Sinclair, B. J., & Renault, D. (2011). Metabolic rate and oxidative stress in insects exposed to low temperature thermal fluctuations. *Comparative Biochemistry and Physiology. Part A, Molecular & Integrative Physiology*, *158*(2), 229–234. https://doi.org/10.1016/j.cbpa.2010.11.007

Lee, K. P., Simpson, S. J., Clissold, F. J., Brooks, R., Ballard, J. W. O., Taylor, P. W., Soran, N., & Raubenheimer, D. (2008). Lifespan and reproduction in drosophila: New insights from nutritional geometry.

Proceedings of the National Academy of Sciences, *105*(7), 2498–2503. https://doi.org/10.1073/pnas.0710787105

Liaqat, W., Altaf, M. T., Barutçular, C., Nawaz, H., Ullah, I., Basit, A., & Mohamed, H. I. (2023). Ultraviolet-B radiation in relation to agriculture in the context of climate change: A review. *Cereal Research Communications*, *1–24*, 1–24. https://doi.org/10.1007/s42976-023-00375-5

Liu, M., Jiang, P., Chase, J. M., & Liu, X. (2024). Global insect herbivory and its response to climate change. *Current Biology*, *34*(12), 2558–2569.e3. https://doi.org/10.1016/j.cub.2024.04.062

Ma, J. F., & Yamaji, N. (2006). Silicon uptake and accumulation in higher plants. *Trends in Plant Science*, *11*(8), 392–397. https://doi.org/10.1016/j.tplants.2006.06.007

Malčovská, S. M., Dučaiová, Z., & Bačkor, M. (2014). Impact of silicon on maize seedlings exposed to short-term UV-B irradiation. *Biologia*, *69*(10), 1349–1355. https://doi.org/10.2478/s11756-014-0432-2

Mao, Y.-B., Cai, W.-J., Wang, J.-W., Hong, G.-J., Tao, X.-Y., Wang, L.-J., Huang, Y.-P., & Chen, X.-Y. (2007). Silencing a cotton bollworm P450 monooxygenase gene by plant-mediated RNAi impairs larval tolerance of gossypol. *Nature Biotechnology*, *25*(11), 1307–1313. https://doi.org/10.1038/nbt1352

Masoumzadeh, A., Hosseininaveh, V., & Ghamari, M. (2017). Impact of carbohydrase inhibition on *Habrobracon hebetor* in a tritrophic diet-host-parasitoid system. *Entomologia Experimentalis et Applicata*, *162*(2), 188–196. https://doi.org/10.1111/eea.12537

Massey, F. P., & Hartley, S. E. (2009). Physical defences wear you down: Progressive and irreversible impacts of silica on insect herbivores. *Journal of Animal Ecology*, *78*(1), 281–291. https://doi.org/10.1111/j.1365-2656.2008.01472.x

Mewis, I., Schreiner, M., Nguyen, C. N., Krumbein, A., Ulrichs, C., Lohse, M., & Zrenner, R. (2012). UV-B irradiation changes specifically the secondary metabolite profile in broccoli sprouts: Induced signaling overlaps with defense response to biotic stressors. *Plant and Cell Physiology*, *53*(9), 1546–1560. https://doi.org/10.1093/pcp/pcs096

Moise, E. R. D., McNeil, J. N., Hartley, S. E., & Henry, H. A. L. (2019). Plant silicon effects on insect feeding dynamics are influenced by plant nitrogen availability. *Entomologia Experimentalis et Applicata*, *167*(2), 91–97. https://doi.org/10.1111/eea.12750

Molyneux, P. (2004). The use of the stable free radical diphenylpicrylhydrazyl (DPPH) for estimating antioxidant activity. 26(2).

Nocchi, N., Duarte, H. M., Pereira, R. C., Konno, T. U. P., & Soares, A. R. (2020). Effects of UV-B radiation on secondary metabolite production, antioxidant activity, photosynthesis and herbivory interactions in *Nymphoides humboldtiana* (Menyanthaceae). *Journal of Photochemistry and Photobiology B: Biology*, *212*, 112021. https://doi.org/10.1016/j.jphotobiol.2020.112021

Ohtsuka, K., & Osakabe, M. (2009). Deleterious effects of UV-B radiation on herbivorous spider mites: They can avoid it by remaining on lower leaf surfaces. *Environmental Entomology*, *38*(3), 920–929. https://doi.org/10.1603/022.038.0346

Oksanen, J., Simpson, G. L., Blanchet, F. G., Kindt, R., Legendre, P., Minchin, P. R., O'Hara, R. B., Solymos, P., Stevens, M. H. H., Szoecs, E., Wagner, H., Bedward, M., Bolker, B., Borcard, D., Carvalho, G., De Caceres, M., Durand, S., Evangelista, H. B. A., Hannigan, G., … Weedon, J. (2025). vegan: Community Ecology Package (R package version 2.7-1). https://CRAN.R-project.org/package=vegan

Prieto-Ruiz, I., Garzo, E., Moreno, A., Dáder, B., Medina, P., Viñuela, E., & Fereres, A. (2019). Supplementary UV radiation on eggplants indirectly deters *Bemisia tabaci* settlement without altering the predatory orientation of their biological control agents *Nesidiocoris tenuis* and *Sphaerophoria rueppellii*. *Journal of Pest Science*, *92*(3), 3. https://doi.org/10.1007/s10340-019-01103-x

Punia, A., & Chauhan, N. S. (2022). Effect of daidzein on growth, development and biochemical physiology of insect pest, *Spodoptera litura* (Fabricius). *Comparative Biochemistry and Physiology Part C: Toxicology & Pharmacology*, *262*, 109465. https://doi.org/10.1016/j.cbpc.2022.109465

Qi, J., Zhang, M., Lu, C., Hettenhausen, C., Tan, Q., Cao, G., Zhu, X., Wu, G., & Wu, J. (2018). Ultraviolet-B enhances the resistance of multiple plant species to lepidopteran insect herbivory through the jasmonic acid pathway. *Scientific Reports*, *8*(1), 277. https://doi.org/10.1038/s41598-017-18600-7

R Core Team. (2025). *R: A language and environment for statistical computing*. R Foundation for Statistical Computing. https://www.R-project.org/

Raubenheimer, D., Simpson, S. J., & Mayntz, D. (2009). Nutrition, ecology and nutritional ecology: Toward an integrated framework. *Functional Ecology*, *23*(1), 4–16. https://doi.org/10.1111/j.1365-2435.2009.01522.x

Reidinger, S., Ramsey, M. H., & Hartley, S. E. (2012). Rapid and accurate analyses of silicon and phosphorus in plants using a portable X-ray fluorescence spectrometer. *New Phytologist*, *195*(3), 699–706. https://doi.org/10.1111/j.1469-8137.2012.04179.x

Reyhani-Haghighi, S., Cazzonelli, C., Hartley, S. E., & Johnson, S. N. (2026). Raw data: Elevated UV-B alters anti-herbivore plant defence allocation, while silicon supplementation maintains resistance. Figshare. https://doi.org/10.6084/m9.figshare.31368490

Robinson, E. A., Ryan, G. D., & Newman, J. A. (2012). A meta-analytical review of the effects of elevated CO_2 on plant–arthropod interactions highlights the importance of interacting environmental and biological variables. *New Phytologist*, *194*(2), 321–336. https://doi.org/10.1111/j.1469-8137.2012.04074.x

Rousseaux, M. C., Julkunen-Tiitto, R., Searles, P. S., Scopel, A. L., Aphalo, P. J., & Ballaré, C. L. (2004). Solar UV-B radiation affects leaf quality and insect herbivory in the southern beech tree *Nothofagus antarctica*. *Oecologia*, *138*(4), 505–512. https://doi.org/10.1007/s00442-003-1471-5

Saxena, I., Srikanth, S., & Chen, Z. (2016). Cross talk between H_2O_2 and interacting signal molecules under plant stress response. *Frontiers in Plant Science*, *7*, 570. https://doi.org/10.3389/fpls.2016.00570

Schaller, J., Brackhage, C., & Dudel, E. G. (2012). Silicon availability changes structural carbon ratio and phenol content of grasses. *Environmental and Experimental Botany*, *77*, 283–287. https://doi.org/10.1016/j.envexpbot.2011.12.009

Shen, X., Li, X., Li, Z., Li, J., Duan, L., & Eneji, A. E. (2010). Growth, physiological attributes and antioxidant enzyme activities in soybean seedlings treated with or without silicon under UV-B radiation stress. *Journal of Agronomy and Crop Science*, *196*(6), 431–439. https://doi.org/10.1111/j.1439-037X.2010.00428.x

Shen, X., Zhou, Y., Duan, L., Li, Z., Eneji, A. E., & Li, J. (2010). Silicon effects on photosynthesis and antioxidant parameters of soybean seedlings under drought and ultraviolet-B radiation. *Journal of Plant Physiology*, *167*(15), 15. https://doi.org/10.1016/j.jplph.2010.04.011

Shi, C., & Liu, H. (2021). How plants protect themselves from ultraviolet-B radiation stress. *Plant Physiology*, *187*(3), 1096–1103. https://doi.org/10.1093/plphys/kiab245

Simpson, S. J., Clissold, F. J., Lihoreau, M., Ponton, F., Wilder, S. M., & Raubenheimer, D. (2015). Recent advances in the integrative nutrition of arthropods. *Annual Review of Entomology*, *60*, 293–311. https://doi.org/10.1146/annurev-ento-010814-020917

Singh, A., Kumar, A., Hartley, S., & Singh, I. K. (2020). Silicon: Its ameliorative effect on plant defense against herbivory. *Journal of Experimental Botany*, *71*(21), 6730–6743. https://doi.org/10.1093/jxb/eraa300

Summers, C. B., & Felton, G. W. (1994). Prooxidant effects of phenolic acids on the generalist herbivore *Helicoverpa zea* (lepidoptera: Noctuidae): Potential mode of action for phenolic compounds in plant anti-herbivore chemistry. *Insect Biochemistry and Molecular Biology*, *24*(9), 943–953. https://doi.org/10.1016/0965-1748(94)90023-X

Sunkar, R., Kapoor, A., & Zhu, J.-K. (2006). Posttranscriptional induction of two Cu/Zn superoxide dismutase genes in Arabidopsis is mediated by downregulation of miR398 and important for oxidative stress tolerance. *The Plant Cell*, *18*(8), 2051–2065. https://doi.org/10.1105/tpc.106.041673

Teramura, A. H., & Sullivan, J. H. (1994). Effects of UV-B radiation on photosynthesis and growth of terrestrial plants. *Photosynthesis Research*, *39*(3), 463–473. https://doi.org/10.1007/BF00014599

Thorne, S. J., Maathuis, F. J. M., & Hartley, S. E. (2023). Induction of silicon defences in wheat landraces is local, not systemic, and driven by mobilization of soluble silicon to damaged leaves. *Journal of Experimental Botany*, *74*(17), 5363–5373. https://doi.org/10.1093/jxb/erad224

Toprak, U., Hegedus, D., Doğan, C., & Güney, G. (2020). A journey into the world of insect lipid metabolism. *Archives of Insect Biochemistry and Physiology*, *104*(2), e21682. https://doi.org/10.1002/arch.21682

Tripathi, D. K., Singh, S., Singh, V. P., Prasad, S. M., Dubey, N. K., & Chauhan, D. K. (2017). Silicon nanoparticles more effectively alleviated UV-B stress than silicon in wheat (*Triticum aestivum*) seedlings. *Plant Physiology and Biochemistry, Effects of Nanomaterials in Plants*, *110*, 70–81. https://doi.org/10.1016/j.plaphy.2016.06.026

Van Soest, P. J., & Jones, L. H. P. (1968). Effect of silica in forages upon digestibility. *Journal of Dairy Science*, *51*(10), 1644–1648. https://doi.org/10.3168/jds.S0022-0302(68)87246-7

Vandegeer, R. K., Cibils-Stewart, X., Wuhrer, R., Hartley, S. E., Tissue, D. T., & Johnson, S. N. (2021). Leaf silicification provides herbivore defence regardless of the extensive impacts of water stress. *Functional Ecology*, *35*(6), 1200–1211. https://doi.org/10.1111/1365-2435.13794

Velikova, V., Yordanov, I., & Edreva, A. (2000). Oxidative stress and some antioxidant systems in acid rain-treated bean plants: Protective role of exogenous polyamines. *Plant Science*, *151*(1), 59–66. https://doi.org/10.1016/S0168-9452(99)00197-1

Villena, O. C., Momen, B., Sullivan, J., & Leisnham, P. T. (2018). Effects of ultraviolet radiation on metabolic rate and fitness of *Aedes albopictus* and *Culex pipiens* mosquitoes. *PeerJ*, *6*, e6133. https://doi.org/10.7717/peerj.6133

Wang, J. W., Zheng, L. P., Wu, J. Y., & Tan, R. X. (2006). Involvement of nitric oxide in oxidative burst, phenylalanine ammonia-lyase activation and Taxol production induced by low-energy ultrasound in *Taxus yunnanensis* cell suspension cultures. *Nitric Oxide*, *15*(4), 351–358. https://doi.org/10.1016/j.niox.2006.04.261

War, A. R., Paulraj, M. G., Ahmad, T., Buhroo, A. A., Hussain, B., Ignacimuthu, S., & Sharma, H. C. (2012). Mechanisms of plant defense against insect herbivores. *Plant Signaling & Behavior*, *7*(10), 1306–1320. https://doi.org/10.4161/psb.21663

Wickham, H. (2016). *ggplot2: Elegant graphics for data analysis*. Springer-Verlag. https://doi.org/10.1007/978-3-319-24277-4

World Meteorological Organization. (2022). *Scientific Assessment of Ozone Depletion: 2022*. Global Ozone Research and Monitoring Project—Report No. 278. World Meteorological Organization.

Xu, C., Natarajan, S., & Sullivan, J. H. (2008). Impact of solar ultraviolet-B radiation on the antioxidant defense system in soybean lines differing in flavonoid contents. *Environmental and Experimental Botany*, *63*(1), 39–48. https://doi.org/10.1016/j.envexpbot.2007.10.029

Yang, C.-L., Meng, J.-Y., Zhou, L., & Zhang, C.-Y. (2022). Induced heat shock protein 70 confers biological tolerance in UV-B stress-adapted *Myzus persicae* (Hemiptera). *International Journal of Biological Macromolecules*, *220*, 1146–1154. https://doi.org/10.1016/j.ijbiomac.2022.08.159

Yao, X., Chu, J., Cai, K., Liu, L., Shi, J., & Geng, W. (2011). Silicon improves the tolerance of wheat seedlings to ultraviolet-B stress. *Biological Trace Element Research*, *143*(1), 507–517. https://doi.org/10.1007/s12011-010-8859-y

Yemm, E. W., Cocking, E. C., & Ricketts, R. E. (1955). The determination of amino-acids with ninhydrin. *Analyst*, *80*(948), 209–214. https://doi.org/10.1039/AN9558000209

Yemm, E. W., & Willis, A. J. (1954). The estimation of carbohydrates in plant extracts by anthrone. *Biochemical Journal*, *57*(3), 508–514. https://doi.org/10.1042/bj0570508

Yoruk, R., & Marshall, M. R. (2003). Physicochemical properties and function of plant polyphenol oxidase: A review. *Journal of Food Biochemistry*, *27*(5), 361–422. https://doi.org/10.1111/j.1745-4514.2003.tb00289.x

Zvereva, E. L., & Kozlov, M. V. (2006). Consequences of simultaneous elevation of carbon dioxide and temperature for plant–herbivore interactions: A metaanalysis. *Global Change Biology*, *12*(1), 27–41. https://doi.org/10.1111/j.1365-2486.2005.01086.x

SUPPORTING INFORMATION

Additional supporting information can be found online in the Supporting Information section at the end of this article.

Appendix S1. UV-B dose rationale and spectral characterisation.

Figure S1. Normalised net spectral irradiance of the three UV-B treatments.

Figure S2. Absolute spectral irradiance of the three UV-B treatments.

Figure S3. Biologically effective spectral irradiance for the three UV-B treatments.

How to cite this article: Reyhani Haghighi, S., Cazzonelli, C. I., Hartley, S. E., & Johnson, S. N. (2026). Elevated UV-B alters anti-herbivore plant defence allocation, while silicon supplementation maintains resistance. *Functional Ecology*, *00*, 1–19. https://doi.org/10.1111/1365-2435.70398